DNA ÄR INTE BARA EN VACKER MOLEKYL - det är även det kemiska ämne som bygger upp vår arvsmassa, vars information i slutändan faktiskt bestämmer det mesta om hur vi är konstruerade och fungerar. För att få en detaljerad bild av hur cellens maskineri läser av instruktionerna som lagras i DNA, eller lära oss hur sjukdomsalstrande gener selektivt kan blockeras, är det vikigt att studera mekanismerna bakom samspelet mellan DNA och andra molekyler.

De ruteniumkomplex jag undersökt skiljer sig från de flesta andra DNA-bindande substanser genom att de binder mycket långsamt men samtidigt mycket starkt till DNA. Det intressanta med studierna som presenteras i avhandlingen är att inbindningshastigheten, kinetiken, dessutom visat sig vara extremt känslig för små skillnader i strukturen hos både DNA och ruteniumkomplex. Exempelvis är hastigheten över tusen gånger högre med DNA som bara innehåller A- och T-baser, jämfört med DNA som även innehåller G och C. Vi ser också stora effekter på inbindningsförloppet till DNA som inte är perfekt basparat, och till supercoilat DNA. Man kan tala om en *kinetisk igenkänning* av särskilda DNA-strukturer. Resultaten öppnar dörrar för nya vägar att uppnå selektiv bindning till DNA, något som man eftersträvar inom utvecklingen av såväl diagnostiska som terapeutiska substanser. Även om vägen dit ännu är lång, kan AT-igenkännande ruteniumkomplex vara intressanta som prototyper för läkemedel mot sjukdomar orsakade av organismer med hög andel A och T i sitt DNA, till exempel de parasiter som ger upphov till malaria och sömnsjuka.

PÄR NORDELL

Kinetic Recognition of Nucleic Acids

2009

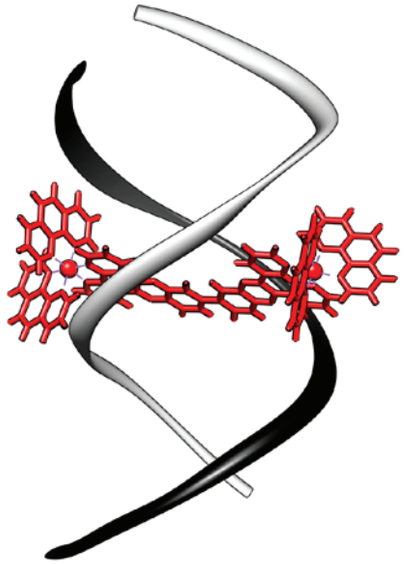

Kinetic Recognition of Nucleic Acids

Studies on the DNA Binding Selectivity of Threading Ruthenium Complexes

PÄR NORDELL

Department of Chemical and Biological Engineering
CHALMERS UNIVERSITY OF TECHNOLOGY
Göteborg, Sweden 2009

THESIS FOR THE DEGREE OF DOCTOR OF PHILOSOPHY

Kinetic Recognition of Nucleic Acids

Studies on the DNA Binding Selectivity of Threading Ruthenium Complexes

PÄR NORDELL

Department of Chemical and Biological Engineering

Chalmers University of Technology

Göteborg, Sweden 2009

KINETIC RECOGNITION OF NUCLEIC ACIDS – STUDIES ON THE DNA BINDING SELECTIVITY OF THREADING RUTHENIUM COMPLEXES

PÄR NORDELL

ISBN 978-91-7385-324-8

Doktorsavhandlingar vid Chalmers tekniska högskola

Ny serie Nr 3005

ISSN 0346-718X

Department of Chemical and Biological Engineering

Chalmers University of Technology

SE-412 96 Göteborg

Sweden

Telephone: +46 (0)31 772 10 00

Printed by Chalmers Reproservice

Göteborg, Sweden 2009

To Märta & Ingmar

Kinetic Recognition of Nucleic Acids – Studies on the DNA Binding Selectivity of Threading Ruthenium Complexes

PÄR NORDELL

Department of Chemical and Biological Engineering
Chalmers University of Technology

ABSTRACT. Despite the great progress in our understanding of DNA during the past half-century, there are many important aspects of its chemical and biological role yet to be explored. The principles by which it selectively interacts with other molecules have attracted much interest due to the relevance for fundamental cellular processes, as well as for the development of diagnostic probes and effective pharmaceutical agents. This Thesis describes the study of the process in which a planar aromatic moiety, hindered by bulky substituents on both ends, is threaded through the DNA double helix. Dumb-bell shaped binuclear ruthenium complexes of the type $[\mu\text{-(bidppz)}(L)_4Ru_2]^{4+}$, L = phenanthroline (**P**) or bipyridine (**B**) bind upon mixing with DNA rapidly on the outside of the double-helix, after which they rearrange to an intercalated binding mode. Passing one large metal centre between the strands requires large transient distortions of the duplex, leading to extremely slow binding kinetics that is sensitive to DNA sequence as well as ruthenium complex structure. This work has (1) addressed the mechanisms behind this "kinetic recognition" and (2) identified potential DNA structural targets.

Both enantiomers of chiral analogues **P** and **B** require several hours at 50°C to rearrange to the threaded binding mode in mixed sequence DNA. Alternating AT polymers, on the other hand, are intercalated within a few minutes at room temperature. The ratio between the forward rates is estimated to vary between 65 (ΛΛ-**P**) and 2500 (ΛΛ-**B**). Studies with AT-tract oligonucleotides show that more than one complete helix turn of AT-DNA is required for efficient threading, a stretch considerably larger than the complexes themselves. Long AT-stretches are however not the only kinetically favored targets; subjecting mixed sequence DNA to negative supercoiling can increase the threading rate by as much as two orders of magnitude. Accelerated intercalation is also observed with partially unpaired DNA. Dissociation from mixed sequence DNA displays half-lives of up to 38 h at physiological temperature, the slowest release reported for a reversibly bound agent. The selectivity demonstrated by the binuclear ruthenium complexes *in vitro* make them interesting in the development of new agents against parasitic protozoa with AT-rich DNA.

KEYWORDS. DNA, ruthenium complexes, intercalation, kinetics, sequence selectivity, supercoiling, spectroscopy, fluorescence, circular dicroism

List of Publications

The Thesis is based on the work contained in the following papers:

I. Mechanism of DNA Threading Intercalation of Binuclear Ru Complexes: Uni- or Bimolecular Pathways Depending on Ligand Structure and Binding Density
Pär Nordell and Per Lincoln*
Journal of the American Chemical Society **2005**, *127*, 9670-9671

II. Kinetic Recognition of AT-Rich DNA by Ruthenium Complexes
Pär Nordell, Fredrik Westerlund, L. Marcus Wilhelmsson, Bengt Nordén and Per Lincoln*
Angewandte Chemie-International Edition **2007**, *46*, 2203-2206

III. Kinetic Characterization of an Extremely Slow DNA Binding Equilibrium
Fredrik Westerlund, Pär Nordell, Bengt Nordén and Per Lincoln*
Journal of Physical Chemistry B **2007**, *111*, 9132-9137

IV. Complex DNA Binding Kinetics Resolved by Combined Circular Dichroism and Luminescence Analysis
Fredrik Westerlund*, Pär Nordell, Julia Blechinger, Teresa M. Santos, Bengt Nordén and Per Lincoln
Journal of Physical Chemistry B **2008**, *112*, 6688-6694

V. DNA Polymorphism as an Origin of Adenine-Thymine Tract Length-Dependent Threading Intercalation Rate
Pär Nordell*, Fredrik Westerlund, Anna Reymer, Afaf H. El-Sagheer, Tom Brown, Bengt Nordén and Per Lincoln
Journal of the American Chemical Society **2008**, *130*, 14651-14658

VI. Supercoil-Accelerated DNA Threading Intercalation
Pär Nordell*, Erik T. Jansson and Per Lincoln
Biochemistry **2009**, *48*, 1442-1444

** Corresponding author*

Contribution report

Paper I	I planned and performed experiments. Main author of the paper.
Paper II	I planned, performed and analyzed most of the experiments. Main author of the paper.
Paper III & IV	Mainly the work of F.W. I contributed to preliminary studies, planning of experiments and writing of papers.
Paper V	I designed, performed and analyzed the kinetic experiments. Main author of the paper.
Paper VI	I designed, performed and analyzed experiments together with E.T.J. Main author of the paper.

CONTENTS

1. INTRODUCTION....1

2. NUCLEIC ACIDS....5

2.1 THE DUPLEX STRUCTURE.... 5
2.2 STRUCTURE AND RECOGNITION OF AT-DNA.... 7
2.3 DNA SUPERCOILING.... 10
2.4 NON-DUPLEX STRUCTURES.... 11
2.5 DNA - LIGAND INTERACTIONS.... 13
2.6 DNA AS THERAPEUTIC TARGET.... 15

3. RUTHENIUM POLYPYRIDYL COMPLEXES....17

3.1 HISTORY AND DEVELOPMENT.... 17
3.2 BINUCLEAR COMPLEXES.... 18

4. FUNDAMENTAL CONCEPTS....21

4.1 ABSORPTION AND EMISSION OF LIGHT.... 21
4.1.1 Photophysics of Ruthenium Polypyridyl Chromophores.... 23
4.2 POLARIZED SPECTROSCOPY.... 23
4.2.1 Linear Dichroism.... 23
4.2.2 Circular Dichroism.... 25
4.3 KINETICS OF CHEMICAL REACTIONS.... 26
4.4 KINETIC MODELLING OF DNA INTERACTIONS.... 28

5. RESULTS....31

5.1 KINETIC CHARACTERIZATION OF THREADING INTERCALATION.... 31
5.1.1 The Uni-Molecular Threading into Alternating AT-DNA.... 31
5.1.2 The Thermodynamics of Threading Mixed Sequence DNA.... 34
5.2 KINETIC SELECTIVITY OF INTERACTION.... 38
5.2.1 AT-DNA.... 38
5.2.2 Unpaired Structures.... 43
5.2.3 Supercoiling.... 45
5.3 EFFECT ON GENE EXPRESSION.... 47

6. CONCLUDING REMARKS....49

7. AUTHOR'S ACKNOWLEDGEMENTS....51

8. REFERENCES....53

1. INTRODUCTION

Life on earth is amazingly diverse. Yet all biological systems, from small bacteria to large plants and animals, are based on the same self-replicating unit, the cell, composed of the same types of molecules organized according to the same fundamental principles. By serving as repository of the genetic information and providing the mechanisms of heredity, deoxyribonucleic acid (DNA) is perhaps the most central constituent of the living cell. The elucidation of the correct double-helical structure by James Watson and Francis Crick in 1953[1] and the presentation of the complete sequence of the human genome in 2001[2] are two of the milestones that during the past half-century not only have revolutionized the understanding of DNA, but also our ability to modify and utilize this information-rich molecule. The implications are seen today in fields of evolutionary biology, genetic engineering, forensic sciences and nanotechnology.

The DNA polymer has an astonishingly simple chemical structure, being a long chain composed of only four types of links, often represented by the letters A, T, C and G. When two complementary DNA molecules hybridize to form the double-helix, an A on one strand is always found opposite a T on the other strand. Likewise, G always pairs up with C. DNA can undergo two major cellular conversions. Before each cell division, the DNA is duplicated through replication, allowing the two new cells to receive a complete set of genetic material. The other main process allows the sequence of the DNA letters to dictate the structure of proteins, the functional components of the cell. Specific segments, the genes, of the DNA are first transcribed into an intermediate, transitory form called ribonucleic acid, RNA. The RNA is subsequently translated into an amino acid sequence, which after folding into the correct three-dimensional structure becomes a functional protein. Despite the advance in our comprehension of replication, transcription and other cellular processes in recent years, there are aspects of which we still have limited understanding, aspects that may be of importance for instance for the identification of new targets for future drugs.

In particular, the chemical and physical factors that direct proteins and small molecules to interact sequence specifically with DNA are important in the development of novel nucleic acid probes and therapeutics against genetic and parasitic diseases. Ruthenium polypyridyl chemistry is attractive in this context since it allows for systematic modification of shape, size and function of candidate molecules. A group of dumb-bell shaped binuclear ruthenium complexes of the type given in Figure 1.1 (centre) have been shown to thread one of its bulky ends through a loophole in the DNA helix to end up in a mechanically “locked” threaded geometry. Threading and unthreading are sterically demanding processes that require large transient openings of the DNA duplex, giving rise to extremely slow binding kinetics, sensitive to DNA target sequence as well as ruthenium centre structure. By conducting detailed *in vitro*

spectroscopic investigations, summarized in this Thesis, we have addressed mechanisms behind this “kinetic recognition” and investigated its usefulness for attaining selective DNA binding.

Figure 1.1 gives an overview of the most important findings. With DNA that contains an even mix of A, T, C and G residues, as for the genomes of most organisms, threading proceeds at a virtually negligible pace at physiological temperature. However, with a synthetic DNA polymer built up by alternating As and Ts only, equilibrium, strongly favoring the threaded state, is established within a few minutes. By studying the increase in luminescence, which accompanies the intercalation process, we have estimated the difference in the forward rate of rearrangement to vary between 65 and 2500 times for four structurally related dimeric ruthenium complexes, showing that even though the AT preference is a general property, it exhibits a great sensitivity towards structural details of the compounds (*Paper II*).

Studies of the interaction with short stretches of DNA with defined sequences further showed that lengthening of an alternating AT-tract from 10 to 14 residues can account for much of the rate leap between mixed sequence and the long alternating AT-DNA (*Paper V*). This is interesting since this is a piece of DNA considerably larger than the dimensions of the complexes themselves, indicating that for this kinetic recognition, the selection mechanisms can extend beyond those of the short-range classical lock-and-key recognition model. AT-rich DNA is found in human pathogens such as the malaria parasite, *Plasmodium falciparum*, and *Trypanosoma brucei*, the parasite causing African sleeping sickness. The targeting of long AT-stretches may provide means to selectively interfere with biochemical pathways of such parasites. Other examples of the sensitivity by which these sterically very challenging ruthenium complexes approach their DNA targets include the accelerated threading at sites where the DNA duplex is unpaired and the way in which the torsional strain of DNA supercoiling can function as a control of threading efficiency (*Paper VI*).

Combination of fluorescence and polarized spectroscopies has revealed that threading into polymeric AT-DNA in general can be described as a uni-molecular rearrangement, giving a direct structure–activity relation for seven different dimeric complexes (*Paper I & IV*). A central and interesting observation is that the rate does not necessarily correlate with the steric bulk of the threading moiety. One may speculate that specific attractive interactions, like hydrophobic contacts, can catalyze the passage of a larger molecular structure through the duplex. The forward threading step constitutes however only one of the two processes that define the interaction. To assess equilibrium parameters kinetics of the reversed unthreading step is also required. The slow release of threaded ruthenium complexes can unfortunately not be accurately probed by conventional surfactant sequestering, which earlier has prevented a full thermodynamic characterization.

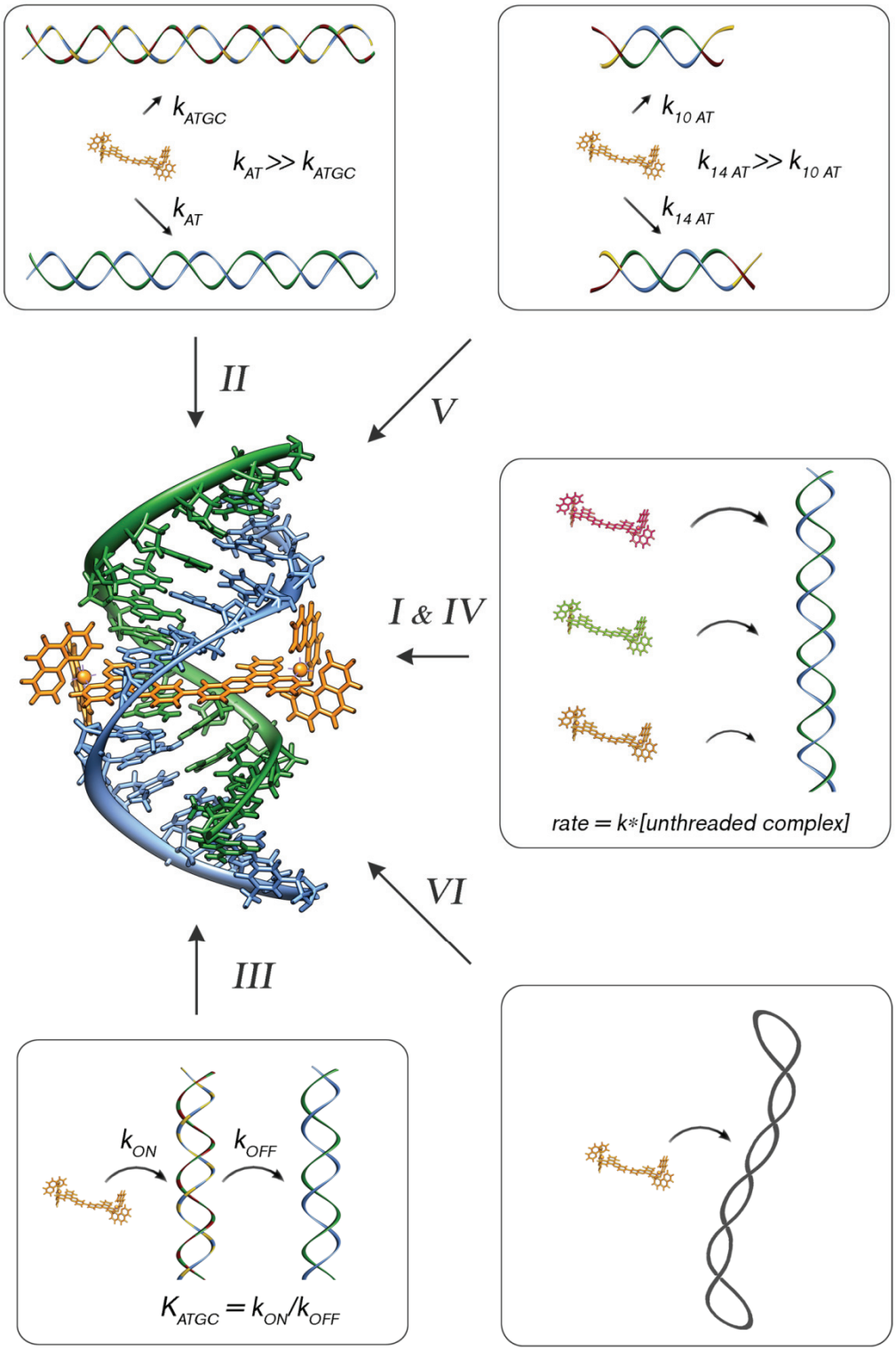

Figure 1.1 Overview of Thesis papers I to VI. Centre: Cartoon depicting a binuclear ruthenium complex threaded into a DNA duplex.

In *Paper III* we report an alternative method, which utilizes the AT-DNA preference, to study the intrinsic dissociation from mixed sequence DNA. The observations again reminded us of the extraordinary properties of the system: unthreading displays a half-life of up to 1.5 days at 37°C - to our knowledge the slowest dissociation reported for a non-covalently bound DNA interacting agent. With access to the dissociation kinetics we obtained a complete thermodynamic profile. It shows that the threading event is an entropically driven process, suggesting that release of water, ordered around the unthreaded complexes, may be a factor that favors the intercalated state.

Before summarizing the results in a more comprehensive manner, this Thesis will give a background to nucleic acids and ruthenium complexes, followed by a brief review of some fundamental concepts.

2. NUCLEIC ACIDS

2.1 The Duplex Structure

The backbone of DNA consists of alternating phosphate and deoxyribose sugar groups, connected via the 5′ and 3′ carbon of the sugar residue. The 1′ carbon is linked to one of four different nucleic acid bases, which together with the phosphate and the sugar forms the repeating units, the nucleotides, in a DNA strand (Figure 2.1a). The bases are adenine (A), guanine (G), cytosine (C) and thymine (T), which are derivatives of purine (A and G) or pyrimidine (C and T).

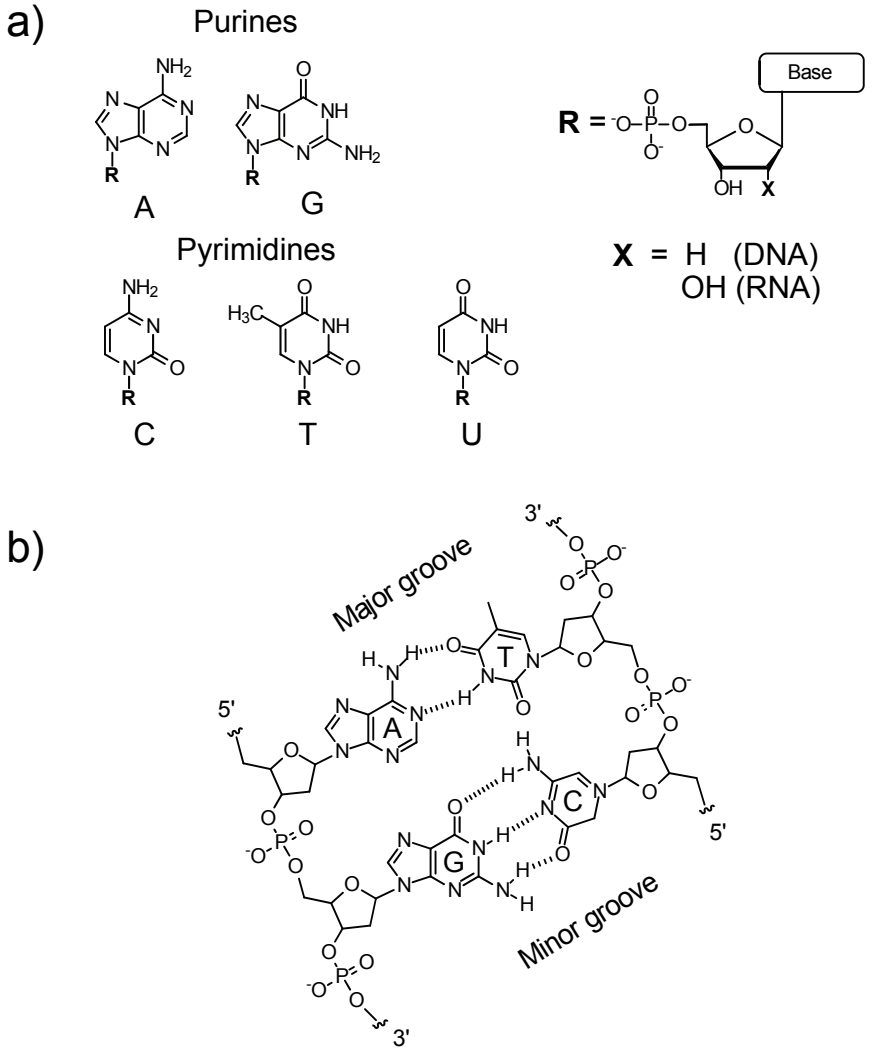

Figure 2.1 (a) The DNA bases adenine (A), guanine (G), cytosine (C) and thymine (T), which together with the phosphate group and deoxyribose sugar form the repeating units in DNA. Uracil (U) replaces thymine in RNA, and deoxyribose is replaced by ribose. (b) The Watson-Crick base-paring scheme. Two hydrogen bonds are formed between A and T, whereas three are formed between G and C.

Two single strands can hybridize to form the characteristic DNA double-stranded helix: two anti-parallel sugar-phosphate backbones wound around each other, with the stacked bases projecting into the interior. According to the Watson-Crick base pairing scheme, a consequence of size and hydrogen bonding pattern of the bases, A pairs up with T and G with C, creating the complementary base pairs (Figure 2.1b). Three hydrogen bonds link G and C, while two are formed between A and T. The stacked neighboring aromatic bases provide a hydrophobic inner environment while the negatively charged phosphate groups, positioned along the outside of the helix, favor interactions with polar surroundings, such as water. Two helical grooves, which expose the edges of the bases, are formed between the intertwined backbones.

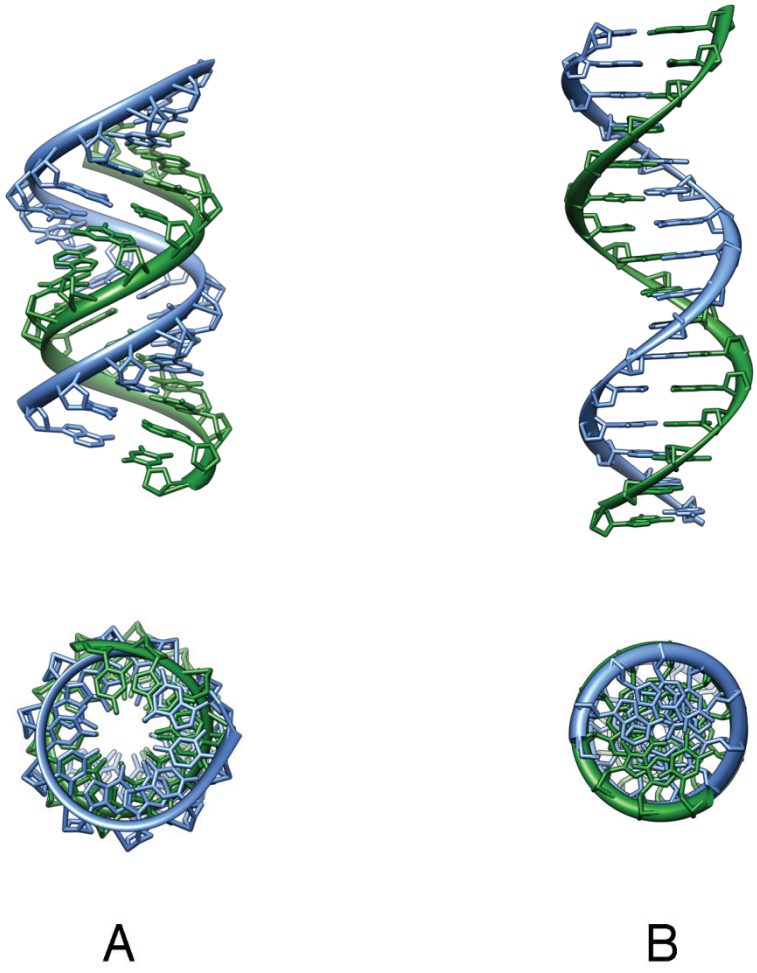

Figure 2.2 Side- and top-view representations of the A and B forms of double-helical DNA, each containing 16 base pairs.

The duplex is polymorphic and adopts the conformation that is most favorable with respect to the character of its surrounding environment, local sequence of bases and interactions with other molecules. In the cell the most abundant conformation is B-DNA (Figure 2.2) where the 3.4 Å thick bases are positioned almost perpendicular to the helix axis. The DNA strands have on average a right-handed twist of 36° per base pair, which

means that the helix will make a complete turn in approximately 10 base pairs. The grooves are distinct; one wide and one narrow, referred to as the major and the minor groove, respectively. At low water activity the DNA helix can adopt the wider and more compact conformation, the A-form. In the A-duplex the stacked bases are strongly tilted and positioned farther from the helix axis, forming a central hollow core. The base pair rise is 2.9 Å and the helix makes a complete turn in 11 base pairs. Double-stranded RNA adopts the A-form, a consequence of the steric restrictions imposed by the presence of a hydroxyl group at the 2′-position of the backbone sugar residue in RNA, ribose. The other structural feature that distinguishes RNA from DNA is that the pyrimidine base thymine is replaced by uracil (U, Figure 2.1a).

2.2 Structure and Recognition of AT-DNA

When Dickerson and colleagues succeeded to crystallize and determine the structure of the first B-DNA dodecamer in the early 1980s,[3,4] it became clear that the DNA is not a completely regular and rigid helix. This and other dodecamers analyzed during the years that followed revealed structures that varied locally depending on the sequence.[5] To date more than a thousand structures of naked and complexed B-DNA sequences have been reported,[6] and even though sequence-conformation correlations have been thoroughly investigated and discussed, translation of the sequential code to a structural code is far from trivial.[7] It is however agreed that AT-rich DNA exhibit characteristic structural and functional features. Factors that are believed to contribute to the differences compared to mixed sequence or GC-rich DNA include (1) the formation of only two hydrogen bonds, which gives A-T base pairs a lower stability and permits a larger twist angle between the base planes of a base pair; (2) the large differences in base stacking of the A/T dinucleotide steps. 5′-TpA-3′ steps have a particularly poor stacking compared to more tightly stacked ApA (=TpT) and ApT; (3) the interlocking of the major groove methyl groups of two successive thymines and the sugar-phosphate backbone, which impose a large conformational restriction on ApA steps.[8]

Differences at nearest-neighbor level may appear subtle, but in runs of A-T base pairs they add cooperatively to promote the formation of particular structural motifs associated with AT-rich DNA. The most general deviation from the canonical B-DNA model is the increased flexibility, usually seen as a narrowing, of the minor groove. In addition, typical structures are known to arise at runs of specific AT sequences. Stretches of more than 4 adenine bases, normally referred to as “A-tracts”, have attracted much attention not only because of their unique local structure, but also due to the effects on the global DNA structure: when positioned in phase with the helical repeat, they cause a macroscopic bending of the DNA. A-tracts are characterized by an unusually high propeller twist, which may permit the formation of bi-furcated hydrogen bonds in the major groove.[9] This has, together with the sterical constraints of the ApA

step mentioned above, in turn been associated with the particular rigidity and inflexibility of A-tracts. Phased A-tracts were first discovered in the sequences of kinetoplast DNA of trypanosomes,[10-12] whose members include pathogens that cause tropical diseases such as African sleeping sickness, Chagas disease and Leishmaniasis. The kinetoplast is a DNA containing structure within the mitochondrion of the parasites. The DNA is organized into a network of thousands of small (commonly 500 to 2500 base pairs long) interlocked DNA circles. The function of the bent A regions remains in many aspects still unclear, but has been suggested to facilitate the compaction of the kinetoplast DNA or to be involved in the recognition by proteins.[13] Stretches of *alternating* adenine and thymine residues are, in contrast to A-tracts, considered flexible and capable of adopting different conformations depending on environment. Crystal structures reveal an oscillating pattern of the helical descriptors, most notably in the twist angle.[9,14] Twist could be thought of as a compromise between optimal stacking of neighboring bases and the constraints of the phosphate backbone. The already efficiently stacked ApT steps increase their overlap (decrease the twist) at the expense of the poorly overlapping TpA steps (with high twist), forming a repeating dimeric unit (Figure 2.3). This type of alternating B-DNA conformation was predicted by Steitz and co-workers for poly(dAdT)$_2$ already in 1979.[15]

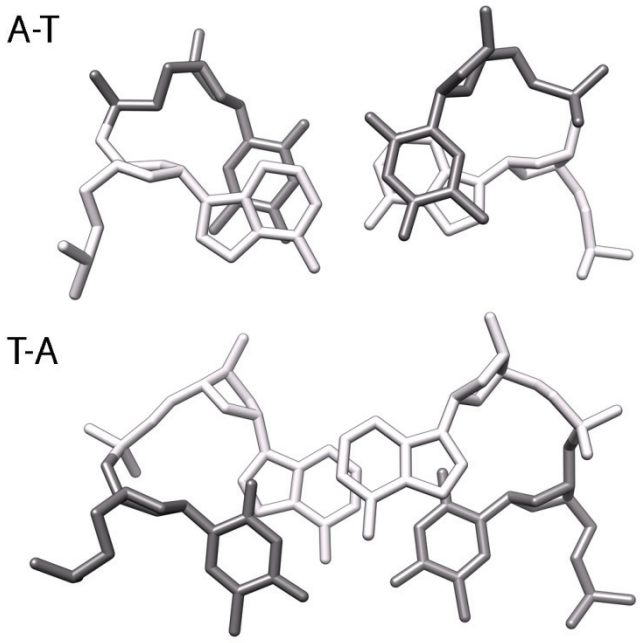

Figure 2.3 Views down the helix axis of dinucleotide steps in the crystal structure a 5′-CGCAT**ATA**TGCG-3′ dodecamer (NDB ID: BDL007).[9] The A(6)-T(7) step (top) has lower twist angle and better overlap than the T(7)-A(8) step.

It is now understood that conformational diversity contributes, together with the direct contacts between amino acids and base pairs down the floors of the grooves, to the recognition between DNA and proteins.[16,17] That the thermodynamic cost of inducing a

structural change in the helix also contributes to sequence recognition is a phenomenon that is well illustrated by the specificity of the TATA box binding protein (TBP).[18-20] Among the first steps in the formation of the transcription initiation complex in eukaryotes is the association of TBP with the TATA box, an AT-rich region with consensus sequence T-A-T-A-A/T-A-A/T/G/C upstream the transcription start within the promoter. TBP specifically binds the minor groove at the TATA box, unwinds and bends the DNA by as much as 80° towards the major groove (Figure 2.4). In prokaryotes the so-called Pribnow box, a highly conserved AT hexamer sequence (consensus sequence T-A-T-A-A-T) located around position -10 relative the transcription start, has a function similar to that of the TATA box. Upon recognition by the RNA polymerase a stretch of this promoter element is strand-separated and bent to form the transcription initiation-ready complex.[21]

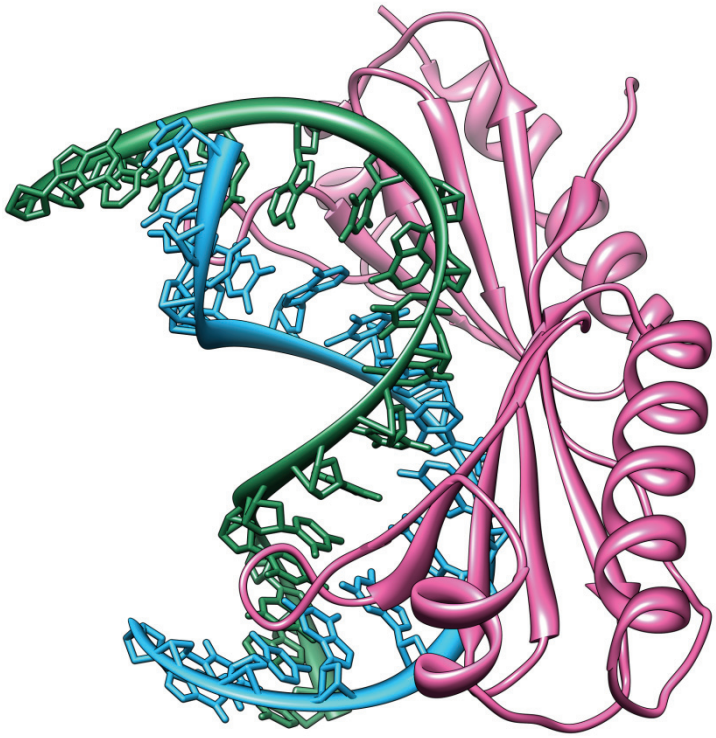

Figure 2.4 Crystal structure of the human TBP core domain/DNA complex, with TBP to the right and the bent 5′-CTGC**TATAAAA**GGCTG-3′ duplex to the left (NDB ID: PDT034).[18]

AT regions also have a functional importance for the initiation of replication. The chromosomal DNA replication in *E-coli* is initiated at a unique sequence, the chromosomal origin of replication, oriC. OriC is an approximately 240 base pair long region including three 13 base pair long AT-rich domains. After binding by initiation enzymes, the DNA is strand separated at the AT-rich regions, forming bubbles which in turn are recognized by helicases that further unwind and strand separate the DNA, before replication proceeds to the elongation phase.[21,22] The examples show how the

indirect readout of a DNA sequence, *i.e.* the conformational adaptivity and stability, contributes to the broad spectrum of interactions observed between DNA and proteins in a cell. It also illustrates how highly conserved AT sequences are recurring at functionally important regions in genomes.

2.3 DNA Supercoiling

Much of the naturally occurring DNA is circular in form. These circles may only be a few thousand base pairs long, as for the kinetoplast mini-circles and the genome of some viruses, or several million base pairs in length, as for the genome of *E-coli*. Most circular DNA is also supercoiled, a high-energy state, first discovered by Vinograd and co-workers,[23] in which the DNA molecule either accommodates too many or too few helical turns per base pair compared to a completely relaxed linear helix. Supercoiling is a topological property that can be described by the linking number Lk, defined as the number of times one backbone strand crosses the surface stretched over the other strand. The linking number of relaxed DNA, Lk^0, will simply be the total number of base pairs N divided by the number of base pairs per turn under a given set of conditions, for instance $Lk^0 \approx N/10.5$ for B-DNA. For $Lk > Lk^0$ supercoiling is positive and for $Lk < Lk^0$ it is negative. The superhelical density σ is a measure of the specific linking difference independent of DNA length

$$\sigma = \frac{Lk - Lk^0}{Lk^0}$$

Intracellular DNA is with few exceptions negatively supercoiled. There are two general forms: the *toroidal*, for which the DNA coils into a series of spirals about an imaginary ring, and the *plectonemic*, for which the DNA crosses over and under itself repeatedly (Figure 2.5).

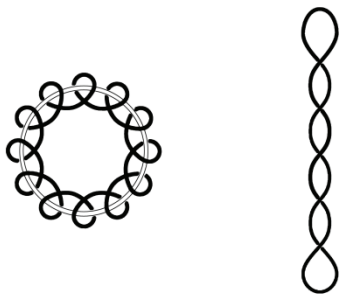

Figure 2.5 Schematic illustration of toroidal (left) and plectonemic (right) DNA supercoiling.

The toroidal arrangement is characteristic for the eukaryotic DNA wrapped around the histone core of a nucleosome. It provides an efficient way of compacting large genomes in the small cell nucleus. Naked DNA, on the other hand, normally adopts the plectonemic form. An interesting consequence of plectonemic supercoiling is

that separated DNA regions are brought into close proximity, potentially forming protein binding sites composed of distal sequences.[24] Examples of such multisite interactions are found in DNA replication, transcription and recombination processes.[25] The geometry can further be described in terms of the relative contributions of twist (Tw) and writhe (Wr) to Lk. Tw reflects how each strand wraps around the helix axis and Wr how the helix coils about itself. As long as the sugar-phosphate backbone is intact, any change in conditions such that for instance Tw changes leads to a compensatory change in Wr, so that $Lk = Tw + Wr$. For example, intercalation of a molecule (see below) between two base pairs which leads to unwinding (decreased Tw), increases the Wr.

The superhelical free energy of circular DNA with $N > 3000$ can be estimated from[26]

$$\Delta G = 10RTN\sigma^2$$

which implies that supercoiled plasmids may have a significant free energy content. For pBR322, a commonly used 4361 base pair long *E-coli* cloning vector, ΔG = 405 kJ/mol at σ = -0.06, and the release of one single helical turn is associated with a $\Delta\Delta G$ of -32 kJ/mol. This is in the order of the ΔG of ATP hydrolysis, the main source of free energy in the cell. Even though the accumulated superhelical energy cannot directly be utilized without introducing backbone scissions, it has fundamental importance in many biological processes. The most prominent effect of negative supercoiling is that it facilitates duplex unwinding, which is necessary in all processes requiring strand separation such as transcription, replication or recombination. At high superhelical density, the additional energy can also result in local transitions to alternative conformations that have a relaxed helicity different from that of B-DNA.[26,27] As such structures only represent a small fraction of the whole molecule (usually < 1% in natural DNA) and exist only under the helical stress of its DNA context, traditional techniques to study DNA conformations (crystallography, NMR and circular dichroism), are generally not applicable. Instead detection has to rely on indirect methods such as mobility shift gel electrophoresis, theoretical predictions and chemical probing. The latter method is based on the increased accessibility to environment, and hence an enhanced reactivity, at the alternative structures. The existence of supercoil-stabilized conformations like cruciforms,[28] left-handed DNA[29] and multi-stranded structures[30] is well established. The biological role *in vivo* is however yet to be clarified.

2.4 Non-Duplex Structures

Deviations from the canonical DNA duplex structures arise in regions where the two strands are non-complementary. Structural irregularities may be categorized as bulge, internal (including single mismatches) or hairpin loops depending on the symmetry and size of the un-paired region (examples in Figure 2.6a-d).[31] In DNA, base

mismatching can result from spontaneous errors in replication or recombination, or be induced by exposure to chemical (*e.g.* DNA-binding agents) or physical (*e.g.* UV-irradiation) mutagens that ultimately may lead to heritable alterations in the genetic material of a cell. The effect of a base pair substitution is dependent on its informational context. Mutations in non-coding regions remain silent, while those in coding regions may have physiological consequences, which in turn is the biological phenomenon driving evolution. Mutations are however unfortunately often harmful to its host organism as displayed by the number of associated degenerative human diseases. Sickle-cell anemia, a blood disorder most commonly occurring in tropical regions, is caused by a single base mutation (A to T) in the β-globin gene, resulting in a substitution of glutamic acid for valine in the β-globin chains of hemoglobin.[32] The cause of cystic fibrosis is mutations in the cystic fibrosis transmembrane conductance regulator (CFTR) gene, of which the most abundant results in deletion of one phenylalanine in the CFTR protein.[33] Mutagenic events are, when left unrepaired, also associated with the development of cancer.[34] While deviations from the regular paired secondary structure in DNA normally are considered abnormalities, they are ubiquitous in RNA and closely associated to its specific structural, catalytic and regulatory functions in the cell. The typical cloverleaf secondary structure of tRNAs, the approximately 80 nucleotides long RNA molecules that transfer amino acids to the growing amino acid chain during translation, comprises, for instance, no less than four helices and three loops (Figure 2.6e).

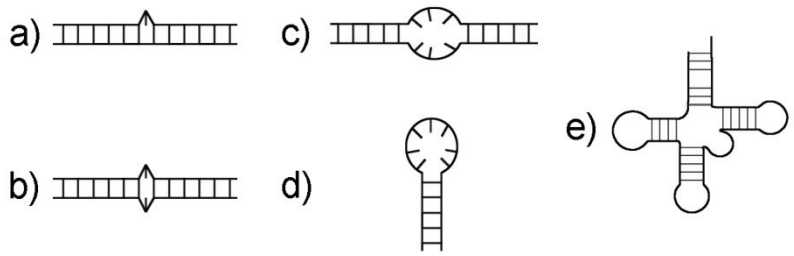

Figure 2.6 Examples of non-duplex structures. Single base bulge (a), mismatch (b), internal (c) and hairpin loop (d). The tRNA structure contains three hairpin loops (e).

The most obvious way in which genetic variation and disease at gene-level can be detected is direct sequencing of the DNA by standard methods. This is however time-consuming and impractical for large-scale sequence analysis. Other methods involve hybridization of a single-stranded probe with the single-stranded target creating a bulge at imperfectly matched base pairs. Such DNA can later be detected through its reduced thermal stability or by retardation gel electrophoresis, in which bulge containing DNA typically migrates slower than fully paired duplexes.[35,36] Development of oligonucleotide microarray technology, in which a large number of fluorescently tagged sequences can be tested against a library of probe sequences, has revolutionized the throughput of genotype variation analysis.[37,38] Still, these procedures all share the problem of finding

stringent conditions for detection of single mismatches in duplexes of different stability, such as A-T and G-C rich DNAs. Methods that recognize *local* structural imperfections constitute an alternative strategy. The particular chemical or conformational properties (*i.e.* backbone perturbations, hydrogen-bonding disruption, base unstacking, base-flipping etc.) of mismatched sites can be utilized as reviewed by Bui *et al.*[39]

2.5 DNA - Ligand Interactions

The residues of a DNA strand are linked into a chain by strong covalent bonds. The three-dimensional conformation is however maintained by much weaker forces including hydrogen, ionic and van der Waals bonds and hydrophobic interactions. These non-covalent interactions account for much of the complex organization and interplay observed in biological systems, like folding and function of proteins and the assembly of plasma membranes. The bond strengths are typically in the order of the average kinetic energy of molecules at physiological temperature, allowing for a continuous disruption and re-formation in various dynamic biological processes. In that manner, non-covalent interactions enable one molecule to bind specifically, yet transiently, to another molecule. Reversible binding of DNA by proteins or small ligands may be divided into three main categories: electrostatic, groove-binding and intercalation. The non-specific association of small positively charged ions (such as Na^+ and Mg^{2+}) to the polyanionic nucleic acid can be considered as purely electrostatic. Electrostatics understandably also plays an important role for the other two more specific types of interaction. Groove-binding refers to the accommodation of a molecule, or a molecular moiety, in the major or the minor groove. Aligning along the groove allows for the formation of specific interactions with several consecutive base pairs, accounting for the significant sequence specificity often exhibited by groove binding agents. The major groove is known to play an important role in DNA-protein interactions, as it is wide enough to dock large structures like α-helices. For smaller molecules, binding in the minor groove is often preferred. Typical minor groove binders are cations of unfused heterocyclics, with inherent rotational freedom to match the helical curvature. Natural antibiotic distamycin[40-42] and synthetic DNA stain DAPI[43-45] (Figure 2.7) are examples of compounds known to bind in the minor groove with a strong preference for AT-rich regions. The specificity is thought to arise from (1) a greater electronegativity of the minor grove at A-T base pairs compared to G-C; (2) the narrow, but adjustable, width that allows a more snuggle fit in AT regions; (3) the exocyclic amino group of guanine protrudes into the minor groove and sterically hinders minor groove binding at G-C base pairs.

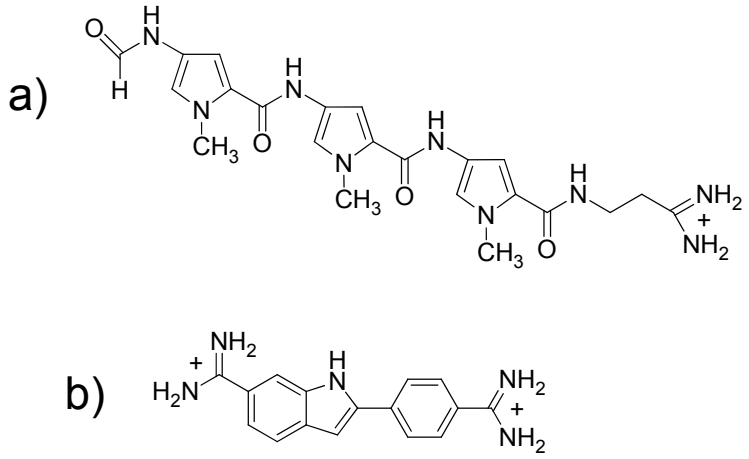

Figure 2.7 The DNA minor groove binders distamycin (a) and DAPI (4′,6-diamidino-2-phenylindole) (b).

Intercalation is insertion of a molecule, or part of a molecule, between two adjacent DNA base pairs. Fused planar aromatic ring systems, such as the classic DNA stain ethidium (Figure 2.8), typically bind by intercalation.[46-49] In early pioneering studies, Lerman discovered that adding the antiviral acridine proflavine to a solution of DNA lead to an increased viscosity, a change he postulated to be a result of a structural perturbation caused by an intercalative binding mode.[50] Intercalation causes indeed unwinding (for ethidium by 26°) around the site of binding and separates surrounding base pairs by approximately one additional base pair spacing.[31] Because of the limited sequence influence on the intercalation pocket itself, simple intercalators generally show little sequence selectivity.[47,51] Specificity can however be increased with additional substituents residing in one of the grooves, as exemplified by actinomycin D.[52,53] Actinomycin is a potent antibiotic known to bind DNA and effectively inhibit RNA synthesis, primarily by interfering with the elongation phase of transcription.[54-56] Variants of the classical intercalation model include bis-intercalation, where the binding agent, exemplified by antitumor drug ditercalinium,[57,58] consists of two intercalating subunits connected by a linker. Another form is *threading* intercalation, for which the insertion is hindered by substituents on both ends of the intercalating ring system. Antibiotic nogalamycin produced by *Streptomyces nogalater* is a well known example of a threading agent found in nature.[59-62] For its anthracycline moiety to be intercalated, either its polar or nonpolar sugar residue has to pass through a sterically restricted loophole in the DNA. For a threading agent with bulky side groups, large transient conformational changes of the double-helix are necessary for formation of the intercalation complex. However, while side groups are obstacles to the passage through the DNA, they potentially have a stabilizing effect on the final intercalated state.[59,63]

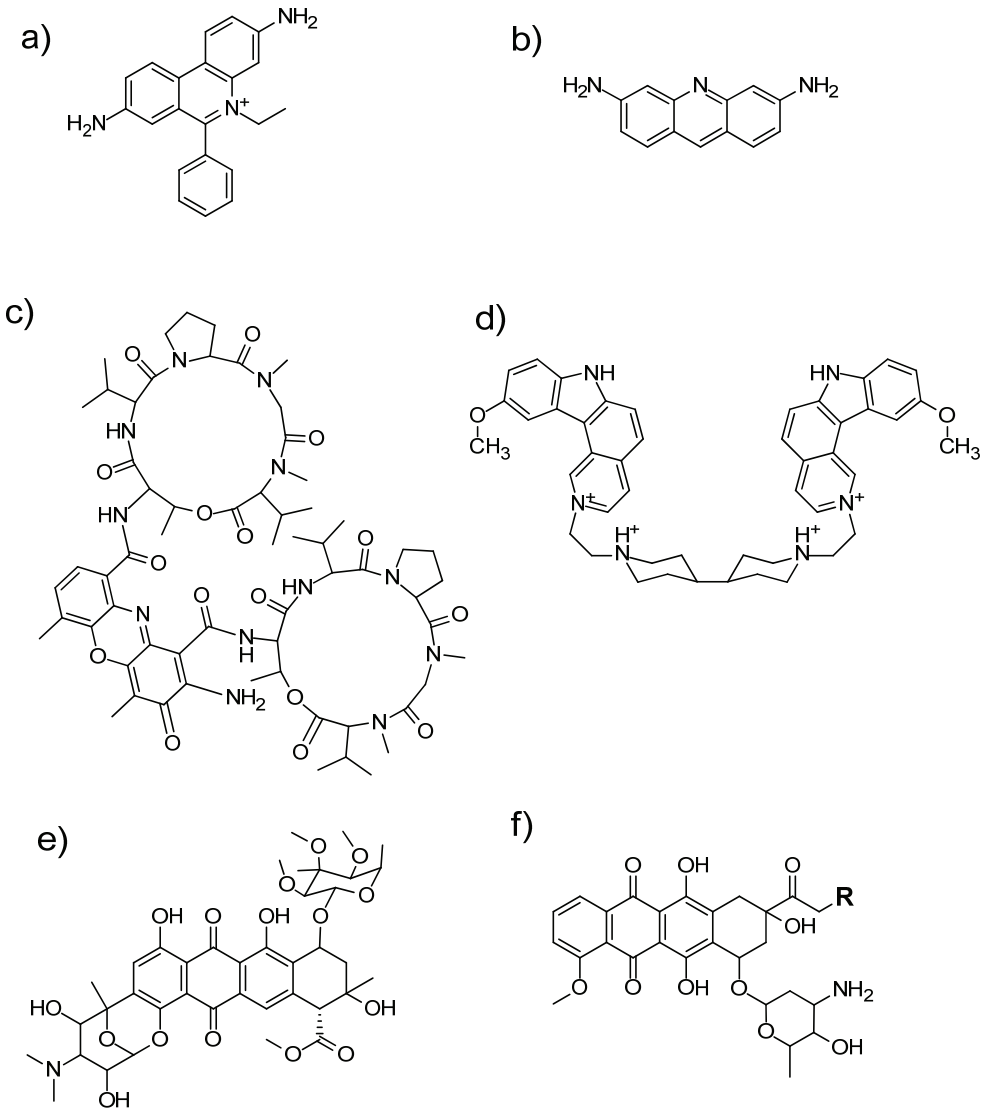

Figure 2.8 The DNA intercalators ethidium (a), proflavine (b), actinomycin D (c), the bis-intercalator ditercalinium (d), the threading intercalator nogalamycin (e) and anti-tumour agents daunomycin (**R** = H) and adriamycin (**R** = OH) (f).

2.6 DNA as Therapeutic Target

In the development of drugs that target the biochemical pathways, small molecules interacting non-covalently with DNA have played an important role. A large portion of these, in particular in the treatment of cancer and infectious diseases, have a natural origin.[64,65] The intercalating anthracyclines daunomycin and adriamycin (Figure 2.8f) are fermentation products of *Streptomyces* bacteria that are approved by the U.S. Food and Drug Administration as anti-tumour agents. Their primary mechanism of cytotoxicity is believed to be mediated by topoisomerase II. Topoisomerases are critical in several DNA processes by creating and rejoining strand breaks. The intercalators act by stabilizing a normally transient intermediate in which the enzyme is covalently linked to the DNA, ultimately leading to double-stranded breaks and cell death. The use of current chemotherapeutics is however limited by

severe side-effects and acquired drug resistance, in turn a result of the inability to target cancer cells specifically. Screening of large combinatorial libraries of synthetic compounds provides one strategy for discovering new potent and selective drugs that act at the DNA level, detailed studies of rationally designed compounds provides another.

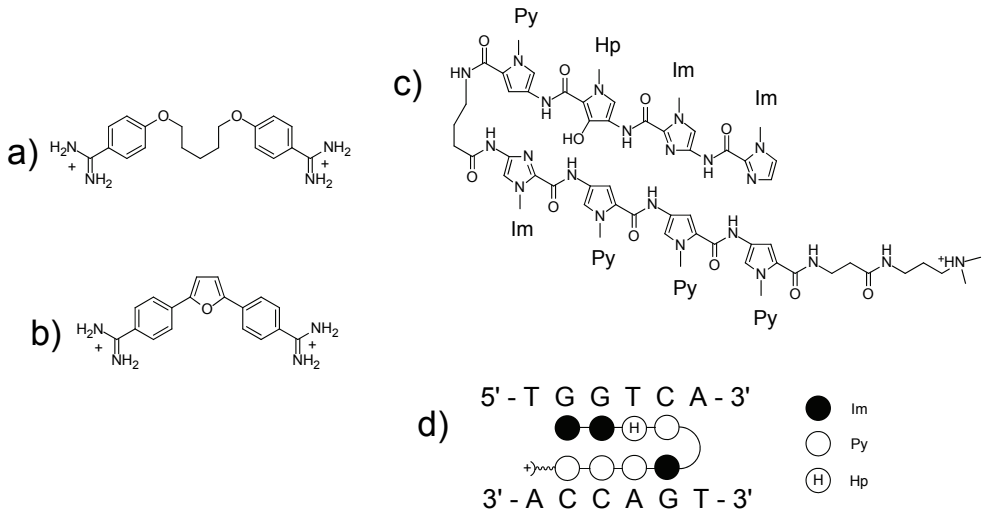

Figure 2.9 Left: AT-selective minor-groove binding agents pentamidine (a) and furamidine (b). Right: Example of an eight-ring polyamide that recognizes a sequence of four Watson-Crick base pairs by formation of a hairpin in the minor groove (c). An imidazole (Im) opposite a pyrrole (Py) recognizes a G-C base pair, Py opposite an Im target C-G base pair, whereas Py/Py paring is degenerate for targeting A-T and T-A. With 3-hydroxypyrrole (Hp) opposite Py, however, T-A can be exclusively targeted, and, vice-versa, Py/Hp targets A-T (d).

Apart from particular base sequences being targets of interaction, natural variations in base content can be exploited for attaining discriminative cytotoxicity. Diamidines constitute a class of AT-selective minor groove binding cations with a long history as antiparasitic agents. Pentamidine (Figure 2.9a) was introduced more than 50 years ago against African sleeping sickness and is, despite high toxicity and development of drug resistance, still used clinically.[66] With furamidine (Figure 2.9b) and other structurally related synthetic compounds, improved antimicrobial activity has been attained.[67-70] When administered intravenously, diamidines spontaneously enter cells and enrich in the mitochondrial kinetoplast, where the thousands of catenated minicircles of high AT content constitute favorable targets. Bound compounds have been suggested to interfere with the complex replication of the kinetoplast DNA, contributing to the observed cytotoxicity.[71] Another example of DNA targeting for therapeutic purposes is the development of hairpin polyamides, compounds that have attracted considerable interest as agents for modulation of gene expression. Discrimination is attained through recognition of Watson-Crick base pairs by a distamycin inspired sequence of pyrrole and imidazole residues (Figure 2.9c).[72-75] By formation of a hairpin that fits the minor groove, polyamides can target any stretch of DNA up to 16 base pairs by side-by-side binding of paired residues (Figure 2.9d).[76] When conjugated to hairpin polyamides, chemotherapeutics of poor selectivity can be guided to a specific gene for down-regulation of transcription for blocking of cancer cell proliferation.[77,78]

3. RUTHENIUM POLYPYRIDYL COMPLEXES

3.1 History and development

Ruthenium complexes first became widely researched during the years that followed the energy crisis in the mid 1970s. The unique photophysical properties of the complex in which a central ruthenium(II) ion coordinates three bipyridine ligands, $[Ru(bpy)_3]^{2+}$, was anticipated to enable it to catalyze photochemical splitting of water into hydrogen and oxygen. Even though efficient hydrogen production by water splitting in practice turned out to be difficult, the investigations formed a basis for much of the use of ruthenium polypyridyl complexes we see today, recently reviewed by Vos and Kelly,[79] in basic and applied research – solar cell applications, molecular electronics, optical sensing and for biomolecular recognition.

Ruthenium polypyridyl complexes as DNA interacting agents is an area of research initiated with the study of $[Ru\mathbf{L}_3]^{2+}$ (**L** = bipyridine (bpy) or phenanthroline (phen), Figure 3.1) by Barton and co-workers more than twenty years ago.[80] Synthetic transition metal complexes may seem an odd choice for studying biomolecules. However, ruthenium polypyridyl complexes possess a number of properties that make them attractive candidates for such applications. Firstly, they are generally chemically inert in the sense that interactions with DNA normally are non-covalent and hence reversible. Further, the inversion-stable octrahedral coordination of the ruthenium ion provides a rigid scaffold around which ligands can be varied for systematic modification of the physical and chemical properties.

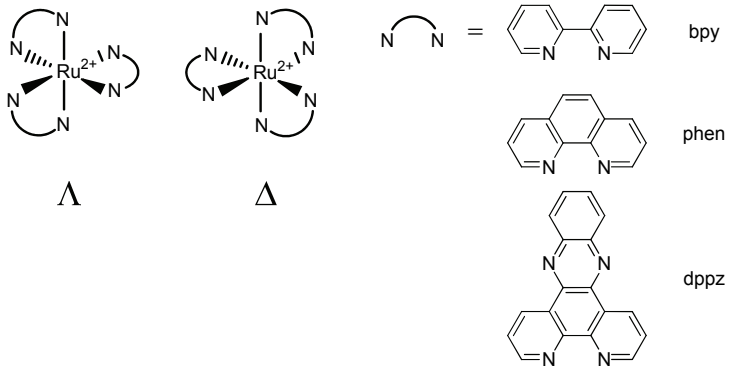

Figure 3.1 Left: the octrahedral coordination of the ruthenium centre gives rise to two stereoisomeric forms, the left-handed (Λ) and the right-handed (Δ) propeller. Right: commonly used bi-dentate ligands: bpy = 2,2′-bipyridine, phen = 1,10-phenanthroline, dppz = dipyrido[3,2-a:2′,3′-c]phenazine.

The metal centres also exhibit an inherent chirality, the right-handed Δ or the left-handed Λ propeller (Figure 3.1), giving rise to handedness discrimination with chiral hosts such as DNA. A final important reason that has motivated the extensive use of ruthenium complexes as DNA probes are their rich photophysical repertoire, in particular the sensitivity of the electronic absorption and emission to different micro-environments.

Studies following the pioneering investigations of $[Ru\mathbf{L}_3]^{2+}$ type complexes came to concern their binding mode. For $[Ru(phen)_3]^{2+}$ it resulted in a discussion spanning several years. Intercalation of one of the phenanthroline ligands as well as both major and minor groove binding was proposed.[81-87] Later studies indicated however that one ligand in fact is partially inserted between two base pairs via the minor groove.[88] Barton and co-workers later started the DNA interaction studies of two analogues, originally synthesized by Sauvage and co-workers,[89] where one of the three ligands had been extended: $[Ru\mathbf{L}_2dppz]^{2+}$ (**L** = bpy or phen) binds strongly by distinct intercalation of its dipyridophenazine (dppz, Figure 3.1) ligand.[90,91] Dppz-based complexes have received special attention as "molecular light-switch" probes. The intercalation of the extended planar ligand between two DNA basepairs is accompanied by a striking increase in luminescence quantum yield. Even though the intercalative binding mode is undisputed, the question whether they are inserted from the major or the minor groove has been open to much debate.[91-95] Dppz complexes are high affinity probes ($K > 10^6\ M^{-1}$ at 50mM NaCl), but display moderate sequence preference ($K_{AT/GC} = 5.9$).[95] While the binding geometry and affinity of the Δ and Λ enantiomer is similar, their photophysical signature differ significantly.[96] Another interesting aspect of the dppz complexes is that binding, unlike binding of many classical intercalators,[97] is entropically driven.[98]

Despite, or as a result of, the controversy that followed the investigations of DNA binding ruthenium complexes, important fundamental knowledge has been acquired over the years. The application of this knowledge is seen today in the development of a new generation of ruthenium complexes, with improved discrimination and function.[99-103] Attention has also been paid to the use of other metals. An example has been reported by Barton *et al*: the steric demand of a bulky, rhodium-based, polypyridyl complex $[Rh(bpy)_2(chrysi)]^{3+}$ (chrysi = chrysene-5,6-quinone diimine) prevents it from intercalating well-matched B-DNA. However, un-pairing at single base mismatches, abasic sites or bulges, allows the chrysi ligand to be inserted.[104,105] Detection is attained by promoting strand cleavage at the binding site by photoactivation and subsequent separation of products by gel-electrophoresis.

3.2 Binuclear complexes

Another development of the field came with studies of binuclear ruthenium complexes, for which improved affinity and chiral discrimination has been attained. In the bisintercalating $[\mu\text{-}C4(cpdppz)_2(phen)_4Ru_2]^{4+}$ (Figure 3.2a), two dppz moieties are

connected via a flexible linker.[106-108] The complex interacts strongly with DNA ($K \approx 10^9$ M^{-1} with calf thymus DNA at 100 mM NaCl), but since association and dissociation involve threading or unthreading of the bulky ruthenium centres through the base stack, the kinetics is much slower than for normal intercalators. The dissociation from calf thymus DNA is multiphasic and requires approximately half an hour to go to completion at room temperature. Of importance is also that while the thermodynamic enantioselectivity is negligible, the effect of chirality on the kinetics is substantial ($k_d(\Delta\Delta)/k_d(\Lambda\Lambda) \approx 0.1$ at 100 mM NaCl). The ΔΔ enantiomer displays, in analogy with nogalamycin,[60,109] much higher association rates with the alternating AT-DNA poly(dAdT)$_2$ than with the alternating GC-DNA poly(dGdC)$_2$, but without effectively increasing the equilibrium binding constant.

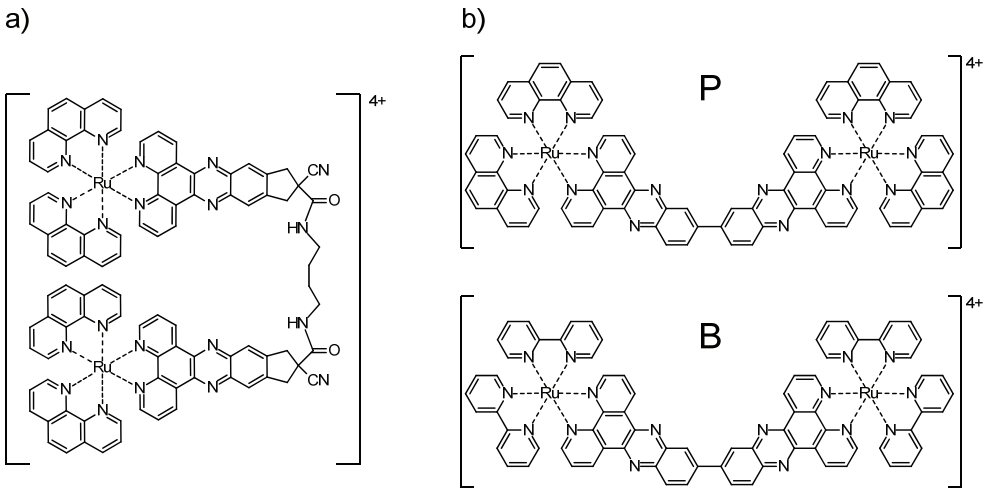

Figure 3.2 Structure of binuclear ruthenium complexes. Bis-intercalating [μ-C4(cpdppz)$_2$(phen)$_4$Ru$_2$]$^{4+}$ (a), and threading [μ-(bidppz)**L**$_4$Ru$_2$]$^{4+}$, where **L** is either phen or bpy (b). C4(cdppz)$_2$ = N,N′-bis(12-cyano-12,13-dihydro-11H-cyclopenta[b]dipyrido[3,2-h:2′,3′-j]phenazine-12-carbonyl)-1,4diaminobutane. Bidppz = 11,11′-bis(dipyrido[3,2-a:2′,3′-c]phenazinyl.

The less flexible analogues [μ-(bidppz)**L**$_4$Ru$_2$]$^{4+}$ (**L** = phen or bpy, complexes hereafter referred to as **P** and **B**, respectively, Figure 3.2b), in which a single bond connects the two monomers, were at first, based on its binding geometry and lack of luminescence, reported to interact with high affinity through binding in one of the grooves ($K \approx 10^{12}$ M^{-1} at 10 mM NaCl).[110] However, later measurements on a sample of ΔΔ-**P** and calf thymus DNA that serendipitously had been left at room temperature for two weeks revealed that the complexes had rearranged to an intercalated, strongly luminescent, mode of binding (Figure 1.1 centre).[111] Constraining the two monomers by shortening the linker had evidently not completely prevented intercalation, only dramatically decreased the rate. Increased temperature and ionic strength increased the rate of rearrangement. Still, at 50°C in 100 mM NaCl equilibrium with calf thymus DNA is not reached until several hours after mixing. It was further shown that the metastable groove-bound form could be rapidly sequestered by addition of surfactant, in sharp

contrast to the threaded form, which required hours at elevated temperature to dissociate. Later the alternative homo-chiral configuration (ΛΛ) and the meso stereoisomer (ΔΛ) of **P** were also shown to intercalate DNA.[112] With alternating AT-DNA poly(dAdT)$_2$, linear dichroism could not distinguish the intermediate groove-bound state. Instead the threaded state was formed already after short equilibration times. The further investigation of this "kinetic recognition" of particular DNA structural features by the sterically very demanding threading ruthenium dimers is the topic of this Thesis.

4. FUNDAMENTAL CONCEPTS

4.1 Absorption and Emission of Light

Spectroscopy, the study of absorption and emission of electromagnetic radiation, *i.e.* light, by matter, is one of the major experimental tools for studies at the molecular level. Electromagnetic radiation of wavelength λ can be thought of as a wave propagating at the speed of light c with an electric and a magnetic field component oscillating in phase at the frequency $\nu = c / \lambda$. The following section gives an introduction to basic concepts of spectroscopic techniques used in this Thesis.

Although light is described as an electromagnetic wave, it is also divided into discrete energy packages, photons, with energy $h\nu$, where h is Planck´s constant. When a molecule in an initial state S_i is exposed to electromagnetic radiation it may absorb a photon and make a transition to a higher-energy final state S_f given that the frequency, ν, of the light satisfies the frequency condition $\Delta E = h\nu$, where ΔE represents the energy difference between the two states. Transitions between electronic states correspond to absorption of ultraviolet and visible light, whereas absorption of longer wavelengths corresponds to transitions between vibrational or rotational states.[113]

The charge distribution in a chromophore gives rise to an electric dipole described by the electric dipole operator $\hat{\boldsymbol{\mu}}$

$$\hat{\boldsymbol{\mu}} = -|e| \sum \vec{\boldsymbol{r}}_i$$

where the summation is over the positions $\vec{\boldsymbol{r}}_i$ of all electrons and e is the electronic elementary charge. In addition to satisfying the frequency condition, in order for a transition to occur the electric field of the light must redistribute the charge density of state S_i as to resemble that of state S_f. If the initial and final states are described by the wavefunctions ψ_i and ψ_f, respectively, a transition between the two results in a transient oscillation described by the transition dipole moment

$$\vec{\boldsymbol{\mu}}_{fi} = \int \psi_f \, \hat{\boldsymbol{\mu}} \psi_i d\tau$$

The transition dipole moment is a vector with a fixed orientation with respect to the molecular framework of the chromophore. The probability for a transition as a result of absorption depends on the magnitude of the transition dipole moment as well as on its orientation relative to the incident light

$$P \propto \left|\vec{\boldsymbol{\mu}}_{fi}\right|^2 \cdot cos^2\theta$$

where θ is the angle between $\vec{\boldsymbol{\mu}}_{fi}$ and the electric field vector. It is practical to talk about the strength of a transition in terms of absorbance, which through the Beer-Lambert law is related to concentration c, the molar extinction coefficient ε_λ, and the optical path length l of a sample

$$A_\lambda = \varepsilon_\lambda \cdot c \cdot l$$

The Jablonski diagram in Figure 4.1 illustrates processes that may follow electronic excitation. The ground, first and second excited states are represented by S_0, S_1 and S_2, respectively. Each state is divided into several vibrational states. A photon of energy $h\nu_A$ is absorbed by a molecule, which is excited from S_0 to a higher electronic singlet state. The molecule is relaxed to the lowest vibrational level of S_1 through vibrational relaxation and internal conversion. The molecule can then return to the ground state S_0 via radiative or non-radiative processes. Radiative relaxation is either accomplished by emitting fluorescence ($h\nu_F$), *i.e.* relaxation directly from the singlet state, or by undergoing intersystem crossing to the first triplet excited state T_1, which can convert to the ground state by emission of phosphorescence ($h\nu_P$).[114]

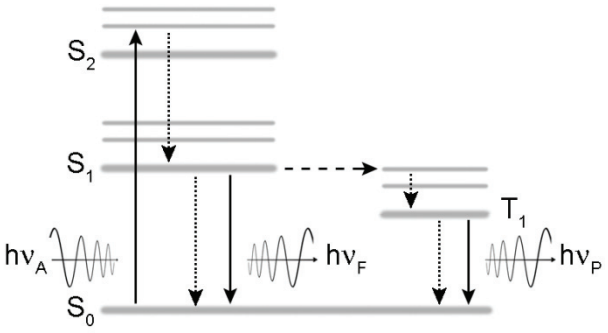

Figure 4.1 Jablonski diagram illustrating the fundamental photophysical processes that follow electronic excitation. Solid arrows indicate radiative processes, dotted vibrational relaxation and internal conversion and dashed intersystem crossing.

Emission of light takes place on a time scale much slower than absorption which allows a wider range of interactions and perturbations to influence the spectrum. As indicated above, different processes compete to depopulate the excited state. The fraction of excited molecules that relax via fluorescence is given by the fluorescence quantum yield

$$\Phi_{\mathrm{F}} = \frac{k_F}{k_F + k_{ic} + k_{is} + k_q(Q)}$$

where k_F , k_{ic} , k_{is} are rate constants for fluorescence, internal conversion and intersystem crossing, respectively, and $k_q(Q)$ describes relaxation through quenching.

4.1.1 Photophysics of Ruthenium Polypyridyl Chromophores

Electronic transitions of ruthenium polypyridyl complex, typified by $[Ru(phen)_2dppz]^{2+}$, can be categorized as being metal-centred (MC), ligand-centred (LC), or to be of metal-to-ligand-charge-transfer (MLCT) character. The absorption spectrum is dominated by the two latter types. $\pi \rightarrow \pi^*$ LC transitions localized on the ligands occur in the UV region, whereas the characteristic orange colour of ruthenium complexes is due to the MLCT transitions at longer wavelengths. A metal d-electron is transferred to a ligand antibonding π^* orbital, creating a charge-separated state of triplet character. The formally forbidden singlet-triplet intersystem crossing is attributed to spin-orbit coupling due to the heavy ruthenium ion. Even though the electron initially can be transferred to any of the coordinated ligands, it is rapidly localized on the dppz ligand which has the lowest lying π^*-orbital. It is believed that the efficient quenching of the luminescence in water and other protic solvents is due to fast hydrogen bonding to the un-coordinated aza nitrogens of the dppz ligand in the excited state.[115,116] Shielding from water in the intercalation pocket of DNA thereby lengthens the excited state lifetime. The accessibility to water has a sensitive dependence on the detailed binding geometry, giving lifetimes and quantum yields that vary strongly with complex structure and DNA sequence.[94,96]

4.2 Polarized Spectroscopy

In the standard absorption measurement isotropic, or non-polarized light is used. Valuable information about the orientation, conformation, size and molecular interactions in a system can, however, be extracted by use of polarized light. Linear and circular dichroism are two techniques based on the differential absorption of polarized light. They constitute two low-resolution complements to the main methods used to obtain structural information, NMR and X-ray diffraction. A full background to theory and applications with emphasis on bio-molecular systems has been given by Nordén and co-workers.[117,118]

4.2.1 Linear Dichroism

The basis for linear dichroism (LD) spectroscopy is the dependence of absorption intensity on orientation of the electric field vector relative to that of the transition dipole moment of a chromophore. It can be used to study systems that are either intrinsically oriented or systems that can be oriented by an external force. The LD of a sample is given by

$$LD = A_{\parallel} - A_{\perp}$$

where $A_{\parallel}$ and $A_{\perp}$ are the absorption of light plane-polarized parallel to and perpendicular to a macroscopic orientation axis, respectively. In a randomly oriented sample LD is zero. Non-zero LD is obtained if the transition dipole moment for a

particular transition is anisotropically oriented, such that the probabilities of absorption of light polarized in the two directions are different. Thus, depending on the magnitude of $A_{\parallel}$ and $A_{\perp}$, the polarization of a given transition can be obtained, and, conversely, if the transition polarization within a molecule is known, information about molecular orientation can be obtained. The reduced linear dichroism LD^r is a dimensionless quantity that only depends on the geometric arrangement of the transition moments relative the orientation axis. It is obtained by dividing the linear dichroism for a given sample and pathlength by the corresponding isotropic absorption

$$LD^r = \frac{LD}{A_{iso}} = 3 \cdot S \cdot O$$

As indicated in the equation above, the LD^r can be interpreted in terms of a product of an orientation factor S and an optical factor O. The orientation factor contains information about the macroscopic level of alignment. $S = 1$ corresponds to perfect parallel orientation of molecules, whereas for a completely randomly oriented sample $S = 0$. For uniaxially oriented "rod-like" molecules, the optical factor may be written

$$O(\alpha) = \frac{3cos^2\alpha - 1}{2}$$

where α is the average angle between the molecular orientation axis and the particular transition dipole moment of interest. The equation illustrates how the optical information always must be interpreted in terms of a cosine squared expression.

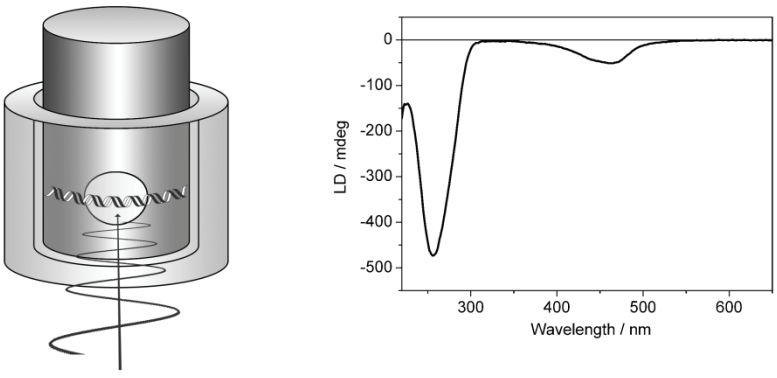

Figure 4.2 Left: In a couette cell the DNA polymers are aligned along the direction of the flow created between an inner fixed and an outer rotating cylinder. Right: Example of a flow LD spectrum of actinomycin D bound to DNA. The DNA bases are oriented perpendicular to the helix axis giving rise to a negative peak in the UV region. In the visible region the phenoxazone chromophore of actinomycin D also gives rise to a negative peak, characteristic for a base co-planar, intercalated binding mode.

Orientation can be attained in stretched polymer films or by aligning molecules along the direction of a field (electric or magnetic) or a flow. Long polymers, such as

DNA, can be efficiently oriented in the flow of a cylindrical Couette cell. The shear gradient between an outer rotating and an inner fixed quartz cylinder orients the DNA helix perpendicular to the rotational axis (Figure 4.2). The in-plane transitions of the DNA bases, oriented almost perpendicular to the helix axis for B-DNA ($\alpha = 90°$), will accordingly give rise to a negative peak in the LD spectrum. Small molecules are not oriented by the flow of the Couette cell. They may however be indirectly oriented if they interact with the aligned DNA host. The LD of a DNA binding drug can further reveal important information about mode of interaction, as exemplified by the sequence dependent binding of the extensively used DNA stain DAPI. The LD of the long-axis transition in DAPI is positive with poly(dAdT)$_2$ and negative with poly(dGdC)$_2$, suggesting a groove bound and intercalated mode of interaction, respectively.[117]

4.2.2 Circular Dichroism

Circular dichroism (CD) is also based on the differential absorption of polarized light. It is defined as

$$CD = A_L - A_R$$

where A_L and A_R is the absorption of left and right *circularly* polarized light, respectively. To measure CD, samples do not have to be oriented, which makes it a more accessible and accordingly more routinely used technique than LD. Instead of orientation, CD is sensitive to the dissymmetry of a system. For circularly polarized light, the field vectors have a constant length, but rotate about their axis of propagation. The electric and magnetic field vectors thus form “chiral” (left or right handed) helices propagating through space. It may then intuitively be realized that left and right handed helices interact differently with chiral samples. More precisely, depending on the handedness of the polarization, the light can couple with interacting electric and magnetic transition dipole moments within a chiral molecule to produce a helical rearrangement of charge. As a consequence, one enantiomer of a chiral molecule will give rise to the mirror image of the CD spectrum of the other enantiomer.

The isolated DNA bases are achiral, as are often DNA binding drugs. Nucleic acids still possess a strong CD signal, which arise predominantly from coupling of the transitions of the helically (chirally) stacked bases in the duplex. The different DNA conformations each have a typical CD signature. Achiral drugs can acquire an induced CD signal (ICD) upon interacting with the DNA by adopting a chiral conformation or from chiral perturbations of its electronic transitions. Observation of ICD is thereby a direct indicator of binding. Structural information can be extracted from the magnitude and shape of the signal. An ICD typical for groove binding is normally an order of magnitude greater than that of intercalation. The formation of dimer, or higher order, complexes in the DNA groove give rise to a strong exciton CD, with a typical bisignate shape.

4.3 Kinetics of chemical reactions

If the conditions for a reaction are suitable for thermodynamic equilibrium to be established fairly rapidly between reactants and products, their free energy relation will determine their relative yield. The decrease in free energy when a product C is formed from the two reactants A and B is given by ΔG in Figure 4.3a. All reactions must however pass one or more transition-states with free energy content higher than that of both reactants and products (illustrated in the figure by the activated complex AB^*). In the late nineteenth century Svante Arrhenius made the empirical observation that the rate constant of many reactions had a temperature dependence of the type $k = A \cdot e^{-E_a/RT}$.[119] The activation energy E_a represents the critical energy which reactants must possess for a reaction to occur, and for a given value of the pre-exponential factor A, the reaction rate decreases with increasing E_a. In transition-state theory, where the normal thermodynamic principles are applied to the activated complex AB^*, the two Arrhenius constants are interpreted in terms of activation enthalpy $\Delta H^{\ddagger}$ and entropy $\Delta S^{\ddagger}$, which in turn can give clues to the molecular factors that control the reaction rate. The activation energy E_a corresponds closely to $\Delta H^{\ddagger}$. Activation parameters are commonly calculated as

$$\Delta H^{\ddagger} = E_a - RT$$

$$\Delta S^{\ddagger} = R \ln \left(\frac{Ah}{kTe}\right)$$

where k and h are the Boltzmann and the Planck constants, respectively.[120] The free energy of activation then follows from $\Delta G^{\ddagger} = \Delta H^{\ddagger} - T\Delta S^{\ddagger}$. Often, in organic-chemical reactions as well as biological processes, this barrier is so high that equilibrium only establishes very slowly and the products in practice attained are those that derive from the lowest activation energy pathway, regardless if this results in the greatest decrease in free energy or not. These reactions are said to be kinetically controlled.

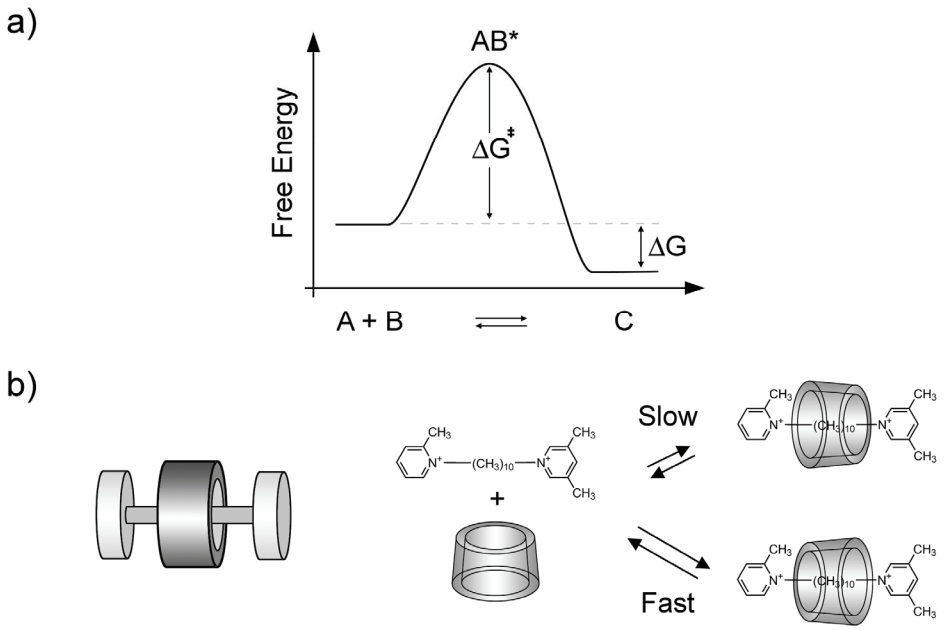

Figure 4.3 (a) Free energy profile for the equilibrium $A + B \rightleftarrows C$. (b) Left: schematic illustration of a mechanically interlocked rotaxane with a cyclic rotor wrapped around a dumb-bell shaped axis. Right: in the kinetically controlled threading of an asymmetric axle through an asymmetric rotor one of the two possible complex face-directions is kinetically favored. (Based on figure in reference[121])

The rearrangement from groove binding to intercalation of the bidppz-bridged ruthenium complexes of the current work is a process strongly dictated by kinetics around room temperature. An example that nicely illustrates kinetic control is found for a completely different, yet principally related molecular system. Rotaxanes constitute a group of mechanically interlocked molecules, often discussed as potential building-blocks in "molecular motors". The name originates from the architecture of its two molecular components: a cyclic *rotor* wrapped around a dumb-bell shaped *axis*. The diameter of the rotor is typically smaller than the ends of the dumb-bell, which prevents fast un-threading. Three routes for constructing rotaxanes are often mentioned. Apart from "capping", for which the bulky stoppers are covalently capped on to the threaded axis, and "clipping", where the rotor is ring-closed around the axis, threading is a possible strategy. Energy barriers for complexation and decomplexation of such a system are understandably very high. Oshikiri *et al.* have made interesting observations in studies of an asymmetric cyclodextrin rotor with an alkyl chain bearing methyl substituted pyridyl end caps as an axle (Figure 4.3b).[121] Firstly, formation of rotaxane complexes is very sensitive to the substitution pattern. Secondly, with asymmetrically substituted pyridyl stoppers two isomers are formed with respect to the face-direction of the axle. However, the rate of formation differs radically. Even 70 days after mixing at 30°C, one of the isomers dominates. To reach equilibrium, at which the yield of both isomers is almost the same, incubation at 70°C for as much as ten days is required.

Accordingly, selectivity, in this case face selectivity, is high at low temperature when the system is kinetically controlled and low at high temperature when the system is thermodynamically controlled. It provides an example of kinetic discrimination and the extremely long times that can be required to reach equilibrium, even for relatively simple, but sterically demanding non-covalent reactions.

4.4 Kinetic Modelling of DNA Interactions

An elegant probabilistic method for modelling non-specific DNA interactions was developed by McGhee and von Hippel in 1974.[122] Traditional representation of ligand binding in the form of Scatchard plots for estimation of binding constants and neighbour exclusion site size fail to adequately describe systems where potential sites for binding can overlap, as the concentration of binding sites then will depend on the distribution of bound ligands. The use of the framework provided by McGhee and von Hippel for analysis of *kinetics* of interactions is demonstrated in *Paper I*. A brief introduction to the method is given below.

The DNA is considered as an infinite one-dimensional lattice of identical repeating residues, normally DNA base pairs. The relative amount of bound ligand is given by the binding density θ defined as the concentration of bound ligand divided by the concentration of total lattice residue. When a ligand binds to the array, n consecutive residues are covered, that is, made inaccessible for other ligands. Saturation of the lattice is consequently attained at $\theta = 1/n$.

The fraction of covered residues on the lattice at a given binding density θ is $n\theta$. Hence, the fraction of free residues is $(1 - n\theta)$. The *conditional* probability that a randomly selected free residue is followed by another free residue is denoted (ff). Equivalently, the conditional probability that a randomly chosen right end of a bound ligand (with the probability $n\theta/n = \theta$), is followed by a free residue is $(b_n f)$. A free residue must have either a free residue or the right end of a ligand to its left hand side, hence

$$1 - n\theta = (1 - n\theta)(ff) + \theta(b_n f)$$

As $(b_n f) = (ff)$ for non-cooperative binding and all possible conditional probabilities must sum up to unity

$$(ff) = (b_n f) = \frac{1 - n\theta}{1 - (n-1)\theta}$$

$$(f b_1) = 1 - (ff) = \frac{\theta}{1 - (n-1)\theta}$$

Now consider a reaction where a ligand in a state A can rearrange to state B (for example groove binding to intercalation). The two states occupy a and b consecutive base pairs, respectively. Then[122]

$$(ff) = \frac{1 - a\theta_A - b\theta_B}{1 - (a-1)\theta_A - (b-1)\theta_B}$$

If the rearrangement between the two states is accomplished uni-molecularly with respect to ligand, but depend on the number x of extra consecutive free residues required in the transition state, the differential rate law below could describe the system:

$$-\frac{d\theta_A}{dt} = \frac{d\theta_B}{dt} = k\theta_A(ff)^x$$

where θ_A and θ_B are the binding densities of states A and B, respectively, and k is the rate constant of the forward step of rearrangement. Given the unknown variables of the rate law (a, b, k and x), the binding density of each specie as a function of time can readily be obtained by numerical integration. If the fraction of ligand in each state can be experimentally determined, for instance by time-resolved absorbance, luminescence or circular dichroism, the neighbour-exclusion site sizes, rate constant and transition-state size can be estimated by fitting the simulated traces to experimental data. Furthermore, if $a = b$, then (ff) will be time-independent and the rate law will be pseudo first-order, but still depend on the mixing ratio $\theta_0 = \theta_A + \theta_B$.

5. RESULTS

The obvious way to follow up the discovery of the slow rearrangement of ΔΔ-**P** was to identify threading structural discriminators of bidppz-bridged dimers. As already mentioned, Wilhelmsson *et al.* reported, soon after the initial finding, that also the meso (ΛΔ) and ΛΛ complexes end up in an intercalated binding mode, in mixed sequence calf thymus DNA as well as in poly(dAdT)$_2$.[112] The dichroism and photophysical studies focused on characterizing the final binding state, but could still reveal large differences in the rate of its formation. An intercalated final binding mode could later also be confirmed for dimers with bipyridine ancillary ligands (**B**). DNA sequence, as well as chiral sense and structure of ancillary ligands, thus appeared to have a larger effect during the actual passage between two DNA base pairs, than on the final mode of interaction, where the bidppz bridge is sandwiched in the base stack and the two metal centers are protruding out from the grooves. At the time when I entered the project, there was anticipation that detailed kinetic information of the threading event with respect to complex structure and base pair context would help to widen our understanding of the mechanism of the discrimination. Below I give a summary of the studies, primarily reported in *Papers I, III* and *IV*, on that topic. Related to this characterization of threading is the identification of potential DNA structural targets, which are reported in *Papers II, V* and *VI* and described in the section after.

5.1 Kinetic Characterization of Threading Intercalation

5.1.1 The Uni-Molecular Threading into Alternating AT-DNA

Following the initial strategy, we started to catalogue threading kinetics by monitoring the increase in luminescence after mixing of four structural analogues (ΔΔ and ΛΛ stereoisomers of **P** and **B**) with mixed sequence DNA and poly(dAdT)$_2$ at different mixing ratios.[123] High-resolution, reproducible kinetic data could be obtained, but although large variations were observed, detailed analysis and interpretation proved not to be straight-forward. Often as many as three exponentials were needed to fit data within acceptable error limits, even with the homogeneous poly(dAdT)$_2$. We were understandably enthusiastic when we eventually found a system where threading appeared to be very simple. At relatively high ionic strength (≥150 mM NaCl), the kinetic trace of ΛΛ-**B** with poly(dAdT)$_2$ could be fitted with a single exponential (Figure 5.1). In addition, data could be fitted with the same rate constant in a wide interval of mixing ratios ([complex]/[base pair] = 1/8 – 1/64). With ΛΛ-**P**, for which the bipyridine ligands have been replaced for phenanthroline, the luminescence evolution could also be described by a 1st-order rate law at the low mixing ratio 1/64. However, with increasing mixing ratios, binding became slower and made a transition to perfect 2nd-order behavior

at [complex]/[base pair] = 1/8. The observations are reported in *Paper I*. The report also includes the global fitting of a kinetic model, based on McGhee and von Hippel conditional probabilities,[122] for the more intriguing behavior of ΛΛ-**P**. A rate law comprising two parallel paths to the intercalated state was constructed. The spatial requirement (free DNA base pairs) of the transition states dictated accessibility of each path, leading to approximate 1st-order behavior at low binding density and 2nd-order kinetics at high binding density. As we later came to understand (see below), the luminescence of the bidppz-bridged dimers is, to varying extent, sensitive to processes that follow the initial threading step, leading us in *Paper I* to propose a more complex mechanism of binding for ΛΛ-**P** than was necessary. Still, the study was important in the sense that we found conditions at which threading could be described as a uni-molecular rearrangement. It also displayed the sensitivity, to be reported in more detail in later papers, of the interaction; in particular the different dependence on mixing ratio and the counter-intuitive property that ΛΛ-**P** threads faster than ΛΛ-**B,** despite the larger steric bulk of its ancillary ligands. The requirement of a surprisingly long stretch of free DNA (more than one complete helix turn of AT base pairs) obtained in the fitted model for ΛΛ-**P** would reappear in later studies with AT-tract oligonucleotides.

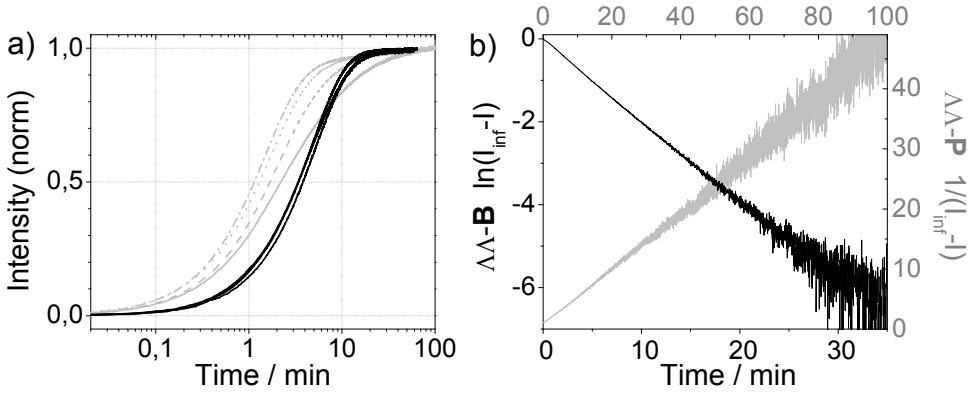

Figure 5.1 Dependency on binding ratio with AT-DNA. (a) Normalized luminescence intensity after mixing poly(dAdT)$_2$ with ΛΛ-**B** (black) or ΛΛ-**P** (grey) at [complex]/[base pair] = 1/8 (—), 1/16 (- -), 1/32 (·····) and 1/64 (-·-) at 25°C. (b) The logarithmic (ΛΛ-**B**) and inverse (ΛΛ-**P**) scale give rise to linear plots at ratio 1/8, showing that the intensity increase follows first- and second-order rate laws, respectively. Note the different x-axis scales. Experiments performed in 150 mM NaCl, 1 mM sodium cacodylate buffer, pH 7.0.

New insights to the interaction with poly(dAdT)$_2$ came with the study of an achiral analogue complex [μ-bidppz([12]aneS$_4$)$_2$Ru$_2$]$^{4+}$ (**S**, Figure 5.2a) with comparably small non-aromatic, sulfur containing ancillary ligands. Intercalation in poly(dAdT)$_2$ could be confirmed by linear dichroism and SDS sequestering measurements (no detectable dissociation 30 min after addition at room temperature). **S** does not exhibit the "light-switch" properties that enable direct probing of interaction from the luminescence. We observed however, as reported in *Paper IV*, that the CD spectrum changed slowly after mixing, on a time-scale comparable to that of the luminescence

evolution of earlier studied dimers. The spectral evolution could further be analyzed by singular value decomposition (SVD), revealing two components well-defined in both the spectral and the time domain. The fastest component required a bi-exponential rate expression to be well described ($\tau_1 \approx 10$ min and $\tau_2 \approx 70$ min at [**S**]/[base pair] = 1/16). For comparison we also monitored the CD evolution of the four previously investigated analogues. SVD analysis showed that one component was enough to describe the spectral changes for these complexes. For ΛΛ-**B** the evolution could as expected be fitted with a single exponential, with a rate constant virtually identical to that obtained from fitting the luminescence trace at the same temperature. To our surprise, however, the spectral evolution of the three other complexes could also be fitted with a single exponential. Global analysis showed that CD and luminescence experimental data could be fitted well with one common and one (ΛΛ-**P** and ΔΔ-**B**) or two (ΔΔ-**P**) additional exponentials covering the slower phases of the luminescence trace. The interpretation we made is that threading of all four analogues in fact can be seen as a uni-molecular rearrangement, described by the CD evolution and the main, fast phase ($\tau \approx 2.3 - 4.4$ min at 25°C, [complex]/[base pair] = 1/16) of the luminescence evolution. The additional complexity of the luminescence data is attributed to a sensitivity of the quantum yield to slowly equilibrating redistributions ($\tau \approx 0.5$ - 10 h) of bound compounds along the DNA. One may speculate that the uni-molecular threading initially gives a stochastic distribution of complexes, whereas at thermodynamic equilibrium they are more clustered.

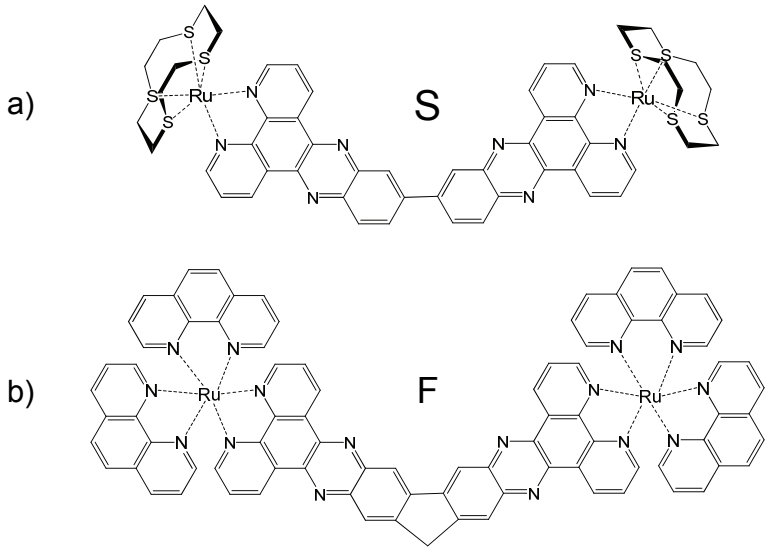

Figure 5.2 Chemical structure of binuclear ruthenium complexes (a) $[\mu\text{-(bidppz)([12]aneS}_4)_2\text{Ru}_2]^{4+}$ (**S**) and (b) $[\mu\text{-(dtpf)(phen)}_4\text{Ru}_2]^{4+}$ (**F**). dtpf = 4,5,9,12,16,17,21,25-octaaza-23H-ditriphenyleno[2,3:b,2,3:h]fluorene.

The study also included the analogue $[\mu\text{-dtpf(phen)}_4\text{Ru}_2]^{4+}$ (**F**, Figure 5.2b) with a completely rigid bridge, for which the binding could be analyzed in a way similar to that for **B** and **P**. Figure 5.3 summarizes globally fitted first inverse rate constants with

poly(dAdT)$_2$ for all studied complexes. **B** and **P** exhibit (with the exception of ΛΛ-**P** at high mixing ratios) similar rates in comparison to **S** and, in particular, **F** ($\tau \approx 17$ min (ΛΛ) and 22 min (ΔΔ)). To conclude, the threading step of **B**, **P** and **F** into poly(dAdT)$_2$ follows 1st-order kinetics and can be described as a uni-molecular rearrangement. Threading of the non-luminescent **S** is more complex, requiring a bi-exponential rate expression. As illustrated by Figure 5.3, the hydrophobicity of the coordinated ion appears more critical to the threading through the base stack, than its size and chirality. Also, rotational freedom of monomers allows a more efficient threading (compare τ of **P** and **F**: ×3.7 (ΛΛ) and ×9.8 (ΔΔ) at [complex]/[base pair] = 1/16).

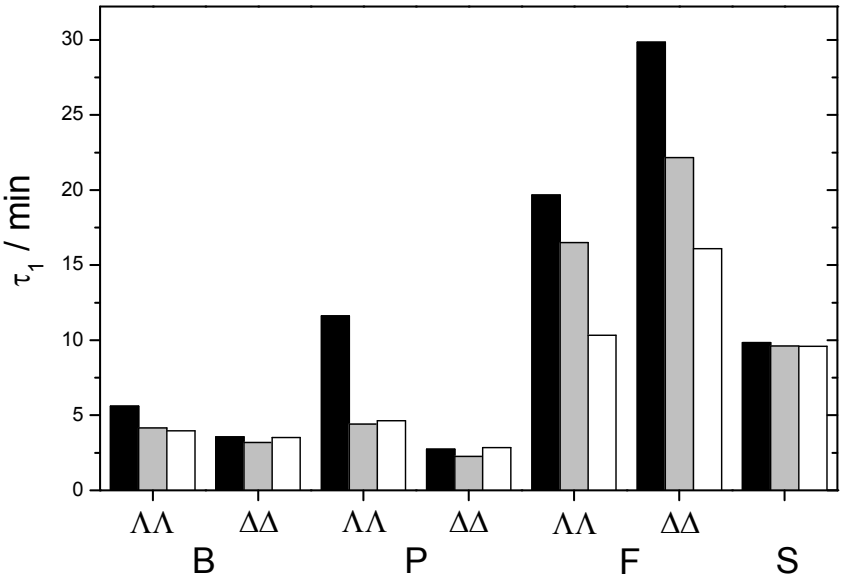

Figure 5.3 The rate of threading AT-DNA. The first inverse rate constant τ_1 obtained from global fitting of CD and luminescence data of the binding of **B**, **P**, **F** (chiral) and **S** (achiral) to poly(dAdT)$_2$ at [complex]/[base pair] = 1/8 (black), 1/16 (grey) or 1/32 (white) at 25°C. For the non-luminescent **S** only CD data was fitted. Experiments performed in 150 mM NaCl, 1 mM sodium cacodylate buffer, pH 7.0.

5.1.2 The Thermodynamics of Threading Mixed Sequence DNA

Normally thermodynamic parameters for DNA–ligand interactions are estimated from experimentally determined equilibrium binding isotherms. Assessing the energetics of the rearrangement from groove binding to intercalation of **P** and **B** is however not straightforward due to the extremely long equilibration times. Thermodynamic parameters can alternatively be determined from kinetic data, which in case of the association event can readily be obtained from the luminescence increase after mixing. A common way to study the dissociation of cationic ligands is to add an excess of an anionic sequestering agent such as SDS to an equilibrated sample of DNA and ligand. SDS forms micelles at concentrations above the CMC, aggregates which act as a hydrophobic sink for ligands free in solution. Addition will accordingly shift the

equilibrium by reduction of the concentration of unbound ligand. As the sequestering is diffusion controlled, the dissociation from the DNA will be the rate limiting event. Electrostatic repulsion has further been assumed to prevent any interaction between SDS and DNA. However, Westerlund *et al.* showed that SDS in fact catalyzes the dissociation of the threading intercalators,[124] making accurate estimation of the intrinsic rate for our system difficult.

Part of the problem was solved when we started to look at competitive binding to calf thymus DNA and poly(dAdT)$_2$, whereupon an alternative way to probe dissociation was discovered. The experiments showed that binding to poly(dAdT)$_2$ was unaffected by the presence of the mixed sequence DNA in the sample. Subsequent SDS induced sequestering of the equilibrated sample resulted in dissociation characteristic for poly(dAdT)$_2$, indicating that complexes were exclusively intercalated in the alternating polymer. The ΔΔ isomers of **P** and **B** have distinctly different luminescence properties in the two types of DNA. The quantum yield of ΔΔ-**P** is 5 times higher in poly(dAdT)$_2$, whereas the emission of ΔΔ-**B** displays a 50 nm red-shift. By utilizing the spectral fingerprints we could conclude that the preference for poly(dAdT)$_2$ not only was kinetic, but also thermodynamic: upon addition of poly(dAdT)$_2$ to a pre-equilibrated sample of complex and calf thymus DNA, the spectrum was slowly shifted to that expected for a sample containing only complex and poly(dAdT)$_2$. Since the association to the AT polymer is much faster (see sections below) than the dissociation from calf thymus DNA, the spectral evolution will furthermore effectively only reflect the non-catalysed rate of dissociation of complexes from intercalation sites in calf thymus DNA. The finding allowed us to assess a complete thermodynamic profile for ΔΔ complexes with calf thymus DNA. The results are reported in *Paper III*, which in addition address the mechanism of catalysis by SDS.

Figure 5.4a shows the obtained calf thymus DNA association and dissociation (poly(dAdT)$_2$ sequestering) traces at three temperatures (47, 52 and 57°C) with ΔΔ-**P** and ΔΔ-**B**. It illustrates the extraordinary properties of the system: ΔΔ-**B** displays a half life of dissociation of 2 h at 50°C. Extrapolated to physiological temperature 37°C (see below) the half life exceeds 18 h. For ΔΔ-**P**, corresponding half lives are around 6 and 35 h, respectively. This is to our knowledge the slowest release reported for a non-covalently DNA-interacting agent. For comparison the prototypical threading intercalator nogalamycin, known for its slow dissociation from DNA, exhibits a half life of about 30 min around physiological temperature.[60]

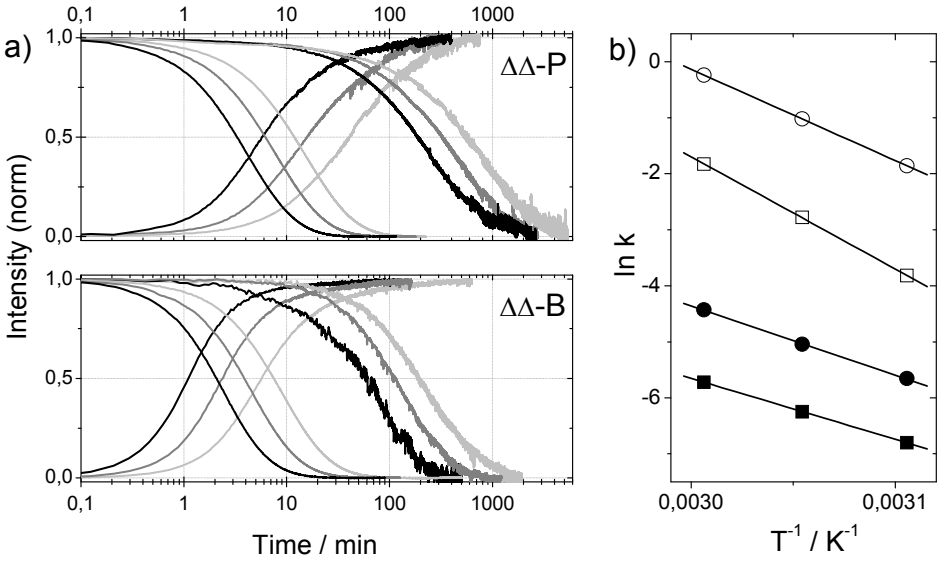

Figure 5.4 Kinetics of interaction with calf thymus DNA. (a) Association and dissociation of ΔΔ-**P** (top) and ΔΔ-**B** (bottom) at 47°C (black), 52°C (dark grey) and 57°C (grey). For the dissociation, probed by scavenging with SDS (14.4 mM, traces to the left) or poly(dAdT)$_2$ (equimolar amount, traces to the right), Y = 0 represent complete sequestering. (b) Arrhenius plots of rate constants obtained from association (open symbols) and dissociation (poly(dAdT)$_2$ sequestering, filled symbols) of ΔΔ-**P** (squares) and ΔΔ-**B** (circles) at the three temperatures. Experiments performed at [complex]/[base pair] = 1/8 in 150 mM NaCl, 1 mM sodium cacodylate buffer, pH 7.0.

Despite the multiphasic nature of the association and dissociation data in the AT system, with ct-DNA a single exponential proved in general to be sufficient to describe 90% of the spectral change well. Fitted rate constants for each event at the different temperatures gave a straight line in an Arrhenius plot (Figure 5.4b), allowing determination of activation energies E_a and the pre-exponential factors. Table 5.1 summarizes acquired activation and equilibrium parameters at 50°C for ΔΔ-**P** and ΔΔ-**B** with calf thymus DNA. The threading process from groove-binding to intercalation is endothermic (by 76 and 33 kJ/mol for ΔΔ-**P** and ΔΔ-**B**, respectively), and hence entropically driven. This thermodynamic pattern (positive enthalpy and positive entropy) is also observed for intercalation of dppz monomers,[98] and typical for hydrophobic interactions, where non-polar residues are made inaccessible to the aqueous environment. The favorable stacking interactions between an intercalated dppz-moiety and the DNA bases are evidently overcome by other molecular interactions, giving a net positive enthalpy change. One may speculate that the disruption of groove-binding electrostatic contacts is less well compensated for with the "non-intercalated" dppz-moiety in a treaded state. The resulting free energy change is similar for the two ΔΔ complexes, around -10 kJ/mol, implying that roughly 1 in 50 complexes remains groove bound at equilibrium at current conditions. The comparably small spectral differences unfortunately make this method less reliable for the ΛΛ complexes. Results indicate however that the ratio is much larger for this series. In this context it should also

be mentioned that both enantiomers of the rigid analogue **F**, which display slower association with poly(dAdT)$_2$ than **B** and **P**, appear not to be able to thread mixed-sequence DNA at all (no quantum yield increase and fast SDS sequestering).

	$\Delta H^{\ddagger}$ (kJ/mol)		$T\Delta S^{\ddagger}$ (kJ/mol)		$\Delta G^{\ddagger}$ (kJ/mol)	
	ΔΔ-**P**	ΔΔ-**B**	ΔΔ-**P**	ΔΔ-**B**	ΔΔ-**P**	ΔΔ-**B**
Threading	164	133	86	60	78	73
Unthreading	88	100	1	17	87	83
	$\Delta H°$ (kJ/mol)		$T\Delta S°$ (kJ/mol)		$\Delta G°$ (kJ/mol)	
	ΔΔ-**P**	ΔΔ-**B**	ΔΔ-**P**	ΔΔ-**B**	ΔΔ-**P**	ΔΔ-**B**
Equilibrium	76	33	85	43	-9	-10

Table 5.1 Activation and equilibrium parameters for ΔΔ-**P** and ΔΔ-**B** threading rearrangement in calf thymus DNA at 50°C. Experiments performed at [complex]/[base pair] = 1/8 in 150 mM NaCl, 1 mM sodium cacodylate buffer, pH 7.0.

It is further worth noticing that while the activation free energy of both threading and unthreading is similar for ΔΔ-**P** and ΔΔ-**B**, the enthalpic and entropic contributions differ considerably. For ΔΔ-**P** the higher forward enthalpy barrier is, compared to ΔΔ-**B**, compensated by a more favorable entropy change. The higher enthalpy barrier observed for the forward association could be expected for the bulkier phenanthroline complex, which intuitively would require a larger transient opening in the DNA duplex. Interestingly, however, in the reversed dissociation process, the smaller bipyridine complex exhibits the highest activation enthalpy barrier. A similar phenomenon is observed for ΛΛ-complexes with poly(dAdT)$_2$; the association activation barrier is much higher for the bipyridine complex (E_a = 132 kJ/mol) compared to the phenanthroline analogue (97 kJ/mol). Again it is apparent that sterical considerations are insufficient to explain the observations. In *Paper II* we suggest that the ability of a large phenanthroline ligand to stack with an unpaired base may be a factor that has a stabilizing influence on the transition state for the ΛΛ enantiomer.

The reversed pattern for association and dissociation in the ΔΔ-series with mixed sequence DNA may further be interpreted in terms of the pre-equilibrium model proposed in *Paper III*, where the rearrangement from groove-binding (G) to intercalation (I) has to pass an intermediate externally bound state (E). The pre-equilibrium between the two unthreaded states (E ⇌ G) is formed instantaneously on mixing, orders of magnitude faster than the threading equilibrium (E ⇌ I). In such a model the overall association activation parameters are dependent on the $\Delta H°$ of the groove-binding pre-equilibrium, and the parameters for dissociation will better reflect the actual threading/unthreading step. The larger difference between ΔΔ-**P** and ΔΔ-**B** in the forward process may then be attributed to the energetics of the groove bound state, for which the accommodation geometry of the two complexes is known to differ significantly. ΔΔ-**P** binds with an angle close to 45° to the helix axis, whereas ΔΔ-**B** in the meta-stable groove bound state is positioned almost parallel to the DNA bases.[110] Irrespective of mechanistic interpretation, it is apparent that the structure of the

ancillary ligands considerably can alter the relative enthalpic and entropic contribution to the activation and equilibrium free energy.

5.2 Kinetic Selectivity of Interaction

The redistribution of threaded complexes from mixed sequence DNA to poly(dAdT)$_2$ shows that the complexes exhibit a strong preference for binding long stretches of alternating AT base pairs. This selectivity of interaction will be the focus of the remainder of the chapter.

5.2.1 AT-DNA

With the discovery that threading into poly(dAdT)$_2$, in sharp contrast to that into natural DNAs, was efficient also at room temperature, came the understanding that the mechanisms of recognition extend beyond those of regular equilibrium binding. If the rearrangement was to be dictated by direct read-out through short-range contacts only, favorable sites would not be infrequent in mixed sequence DNA. The kinetic preference for polymeric AT-DNA is reported in *Paper II*, results which are followed up in *Paper V* with studies with AT-tract oligonucleotides.

As mentioned earlier, [Ru(phen)$_2$dppz]$^{2+}$ displays a weak preference for AT-DNA ($\Delta\Delta G^\circ$ = -4.3 kJ/mol) and only a slightly higher affinity for the Δ enantiomer with calf thymus DNA ($\Delta\Delta G^\circ$ = -1.6 kJ/mol).[95,98] Figure 5.5 shows the dramatic increase in discrimination that results from connecting two dppz monomers to a bidppz complex. While both enantiomeric forms of **P** and **B** intercalate poly(dAdT)$_2$ within a few minutes at 25°C, binding to calf thymus DNA at 50°C requires very long equilibration times and displays a much greater variation. In the Δ-series **B** intercalates faster than **P** (as estimated from half life of intensity increase: $t_{1/2}$ = 11 min and 45 min, respectively). In the Λ-series the difference is larger, but intriguingly with opposite order ($t_{1/2}$ = 132 min and 6 min for ΛΛ-**B** and ΛΛ-**P**, respectively). Two things are worth noting. Firstly, the sequence context plays the most important role, but again it is evident that specific contacts with intercalating complexes also influence the threading step. Secondly, with calf thymus DNA, for which threading is a very improbable event, the structural discrimination is much stronger. The activation energies for ΛΛ complexes with poly(dAdT)$_2$ mentioned above could also be used to extrapolate kinetic traces for binding, permitting a direct comparison to calf thymus DNA binding at 50°C. For ΛΛ-**B** the $t_{1/2}$ ratio for association exceeds three orders of magnitude (~2500), whereas the ratio for ΛΛ-**P** is less extraordinary, around 65. Although the more complex kinetics of the ΔΔ-complexes with AT-DNA precluded a reliable extrapolation to 50°C, the activation parameters obtained for the ΔΔ-complexes with calf thymus DNA could be used to assess a rough $t_{1/2}$ ratio at 25°C. The ratio for ΔΔ-**P** estimated from such extrapolation is almost as large as that for ΛΛ-**B**, whereas that for ΔΔ-**B** is similar to that for ΛΛ-**P** ($t_{1/2}$ ratio of 1600 and 65, respectively, see Table 5.2).

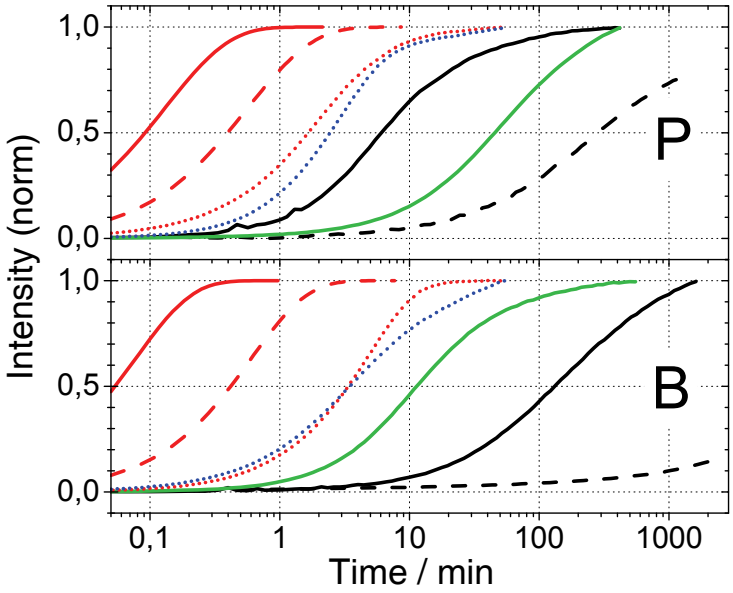

Figure 5.5 Kinetic discrimination between AT and mixed sequence DNA. Intercalation kinetics of **P** (upper panel) and **B** (lower panel) at 50°C (—), 37°C (--) and 25°C (····). Colour coding: ΛΛ binding to poly(dAdT)$_2$ (red), calf thymus DNA (black); ΔΔ binding to poly(dAdT)$_2$ (blue) and calf thymus DNA (green). With calf thymus DNA at 37°C the final intensity was determined after further 18 h at 50°C. For poly(dAdT)$_2$ the 37°C and 50°C curves of the ΛΛ complexes were calculated by using obtained activation energies (see text). Experiments performed at [complex]/[base pair] = 1/16 in 150 mM NaCl, 1 mM sodium cacodylate buffer, pH 7.0.

Complex	Threading Calf thymus DNA (50°C)	Threading Poly(dAdT)$_2$ (25°C)	Ratio
ΛΛ-**B**	132	3.4	2500[a]
ΛΛ-**P**	6.1	1.8	65[a]
ΔΔ-**B**	11	3.9	1600[b]
ΔΔ-**P**	45	2.8	65[b]

Table 5.2 Approximate half life (min) of ruthenium complex threading determined from luminescence intensity increase after mixing with calf thymus DNA at 50°C or poly(dAdT)$_2$ at 25°C. [a]Half life ratio determined from extrapolation of poly(dAdT)$_2$ kinetics to 50°C. [b]Half life ratio determined from extrapolation of calf thymus DNA kinetics to 25°C. Experiments performed at [complex]/[base pair] = 1/16 in 150 mM NaCl, 1 mM sodium cacodylate buffer, pH 7.0.

The threading agent nogalamycin also intercalates at a higher rate (50 times) at AT-sites compared to GC-sites. However, as the dissociation rate is also higher (160 times), the antibiotic actually exhibits a preference for GC-DNA at equilibrium.[59,60] Even though we are unable to measure intrinsic dissociation rates from poly(dAdT)$_2$, we know that the dimers indeed have a strong thermodynamic preference for poly(dAdT)$_2$ as shown in the competition experiments described earlier. The relatively small differences in SDS induced dissociation kinetics between poly(dAdT)$_2$ and ct-DNA

further indicate that, even if rates are severely overestimated, that this preference mainly reflects differences in the association rate.

In *Paper II* we also included a preliminary study with AT-tract oligonucleotides. The results indicated that a surprisingly long stretch of AT base pairs was required for efficient threading. This phenomenon was studied in detail in *Paper V*, where we reported the binding to a series of HEG-linked hairpin oligonucleotides containing a central tract of 6 to 44 AT base pairs flanked by GC-ends (5´-CCGG**X**GGCC-HEG-GGCC**X**CCGG-3´, **X** = $(TA)_3$ to $(TA)_{22}$, where TA indicates T-A base pair followed by a A-T base pair and HEG = hexaethylene glycol). The HEG link has a stabilizing effect on the duplexes, allowing studies at elevated temperature, and made the melting temperature practically invariant of oligonucleotide length ($T_m \approx 66°C$ for the whole series).

Traces obtained at 37°C for **B** and **P** in ΔΔ and ΛΛ conformations with hairpins having 10, 14 and 22 AT base pair tracts are given in Figure 5.6, together with the traces for DNA polymers poly(dAdT)$_2$ and calf thymus DNA. For the shorter 6 base pair tract, we observed low and unaltered emission, indicative of inefficient threading. Increasing the length to 10 base pairs gave a very slow increase, with rate comparable to that with calf thymus DNA. It should be noted that the differences among analogues are conserved, with ΛΛ-**P** exhibiting a considerably faster equilibration time ($t_{1/2} \approx 20$ min) than ΛΛ-**B** ($t_{1/2} \approx 5$ h).

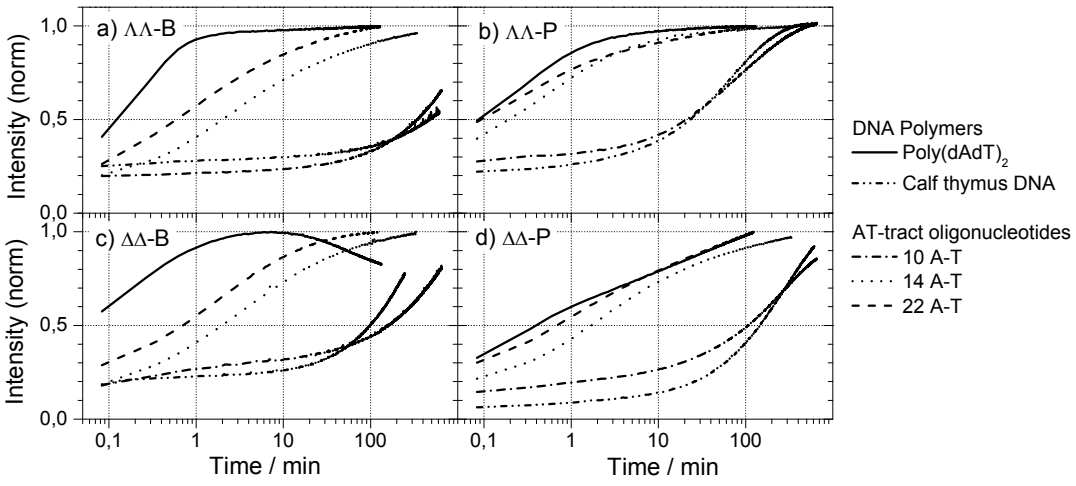

Figure 5.6 AT-tract length dependence of threading. Luminescence after mixing (a) ΛΛ-**B**, (b) ΛΛ-**P**, (c) ΔΔ-**B** or (d) ΔΔ-**P** with DNA polymers or HEG-linked oligonucleotides at 37°C normalized to final/maximum intensity. Coding as indicated in figure. Concentrations: [HEG-linked duplex] = 1 μM, [Ru-complex] = 1 μM, [polynucleotide bases] = 36 μM. Experiments performed in 150 mM NaCl, 1 mM sodium cacodylate buffer, pH 7.0.

The most spectacular effect was however observed when the tract length was increased by another four base pairs: with the 14 AT base pair tract, the half completion times for the four complexes decreased by a factor between 65 (ΔΔ-**P**) and 180 (ΛΛ-**B**), approaching those obtained with the AT polymer. Further increase in tract length to 22 base pairs only moderately increased the rate. Evidently, in terms of the association kinetics, 10 to 14 AT base pairs is a critical interval for efficient threading.

The dissociation process for the AT-tract oligonucleotides could also be successfully monitored by poly(dAdT)$_2$ sequestering. In contrast to the almost 2 orders of magnitude difference in the forward threading rate for ΔΔ-**P**, the rate of unthreading was only slightly affected in the critical length interval. With $t_{1/2}$ of around 1 h for both 10 and 14 AT-tracts at 50°C, the dissociation process is around 5 times faster than with calf thymus DNA. By studying a hairpin duplex that had been cyclized by a copper-catalyzed "click" reaction, we could rule out any mechanism depending on the fraying end as a route to the intercalated state with GC-flanked AT-tracts. We also verified that the "rate leap" was insensitive to mixing ratio and temperature. An interesting observation is that even with a 44 AT base pairs tract, the luminescence increase does not completely mimic that for poly(dAdT)$_2$. In particular, the increase is not monophasic with ΛΛ-**B**. SVD analysis of the CD spectral evolution also reveals a more complex mechanism of binding than for the AT polymer. The CD spectral signature is however similar whether threading into the oligonucleotides, poly(dAdT)$_2$ or calf thymus DNA (Figure 5.7).

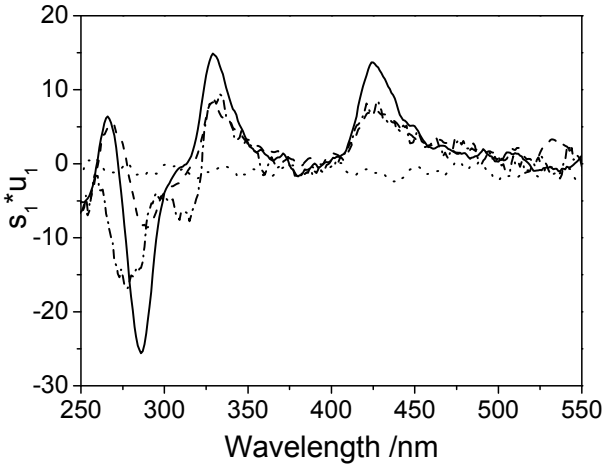

Figure 5.7 Induced CD signature in different DNAs. Main spectral component u_1 multiplied by its weight s_1 for ΛΛ-**B** binding poly(dAdT)$_2$ (—) at 25°C, oligonucleotide with 22 (– –) or 6 (·····) A-T base pairs at 25°C, or calf thymus DNA (–·–) at 50°C. With 6 A-T base pairs no structured spectral component could be obtained even after the temperature was increased to 50°C for several hours. Concentrations: [Ru complex] = 2 μM, [HEG-linked duplex] = 2 μM, [polynucleotide bases] = 72 μM. Experiments performed in 150 mM NaCl, 1 mM sodium cacodylate buffer, pH 7.0.

The alternating AT sequence pattern appears important for effective threading. With an "A-tract" oligonucleotide containing 14 successive adenine bases, a slower and

weaker luminescence increase is observed with ΔΔ-**P**, compared to that for the alternating tract of the same length, and after equilibration, complex is sequestered by SDS 10 times faster (Figure 5.8). Very quick sequestering is observed with tracts of alternating GC base pairs, sequences for which mixing with complex does not result in a luminescence increase, indicating that threading is practically completely prevented in such DNA (unpublished results).

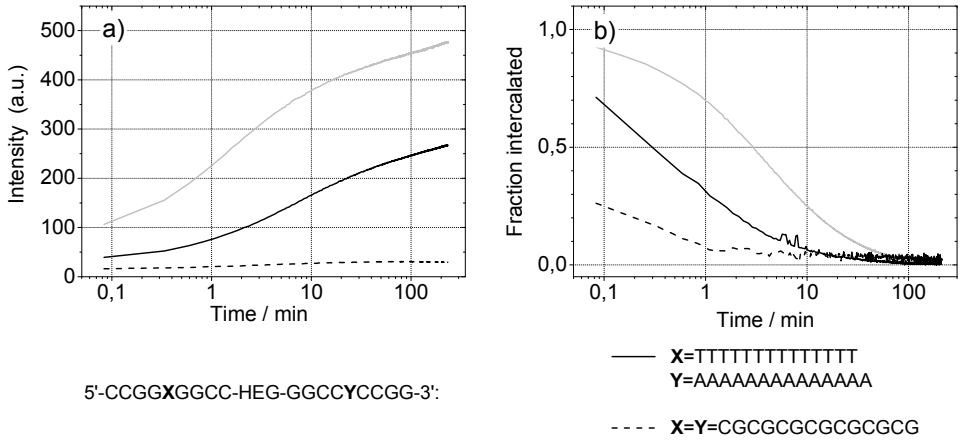

Figure 5.8 Interaction with "A-tract" and GC-DNA. (a) Luminescence intensity after mixing ΔΔ-**P** and HEG-linked oligonucleotides at 37°C. (b) SDS (0.6 wt%) sequestering at 37°C after equilibration for 24h. Y = 0 represent complete sequestering. Coding as indicated in figure. Alternating 14 A-T base pair tract added for comparison (grey). Concentrations: [HEG-linked duplex] = 1 μM, [Ru complex] = 1 μM. Experiments performed in 150 mM NaCl, 1 mM sodium cacodylate buffer, pH 7.0.

Optical tweezers stretching of DNA in the presence of ΔΔ-**P** has recently indicated that threading may not require the opening of more than a single base pair.[125] Still it is evident that a much longer stretch of base pairs influences the barrier to threading between the DNA strands. The thermal stability of duplexes is a cooperative property that could be envisaged to communicate distant sequence information, but melting temperatures of the alternating AT hairpins studied here are very similar. In *Paper V* we instead propose a pre-equilibrium model involving a change of the conformation around the site of interaction to account for the difference between 10 and 14 AT base pairs. The model, outlined in Figure 5.9, is based on the experimental findings that (1) a DNA stretch considerably larger than the dimensions of the compound itself is involved; (2) threading occurs at alternating AT-stretches, sequences known to be especially deformable;[126,127] (3) the similar dissociation rates. From computational models of the final intercalated geometry it seems likely that an intact B-DNA conformation cannot accommodate both $Ru(phen)_2$ moieties ideally. A wider, A-DNA-like, conformation would presumably provide the non-intercalated moiety more favorable electrostatic contacts with the backbone (see figure).

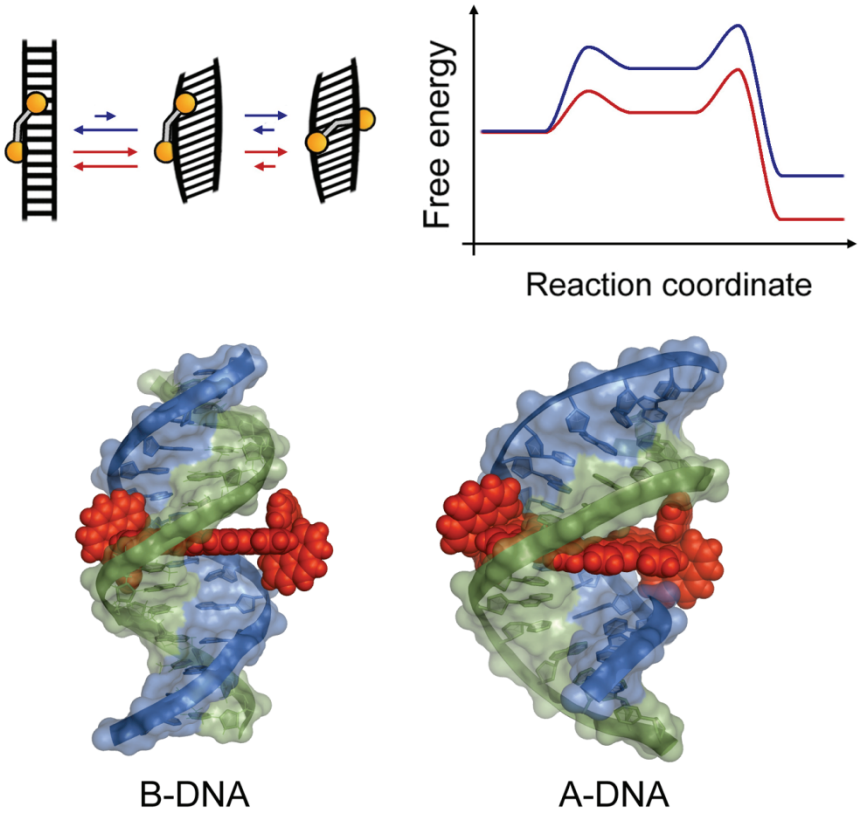

Figure 5.9 Top: Schematic depiction of model of interaction with AT tract oligonucleotides. When a complex associates with the DNA it may, being rigid and highly charged, induce a structural change of the duplex. The energy cost of locally distorting the native DNA conformation will be dependent on the size of the tract. With a longer tract the junction tension to the unperturbed ends will be distributed over more easier-deformable AT base pairs. The subsequent threading step is predominantly affected by base pairs in close contact with the complex. As a consequence, the rate of formation of a threaded state is limited by both the pre-equilibrium between two DNA conformations and the actual threading between the DNA strands, while the rate limiting step of dissociation is unthreading only. Assuming the pre-equilibrium, but not the threading step, to be dependent on the AT tract length increase from 10 (blue) to 14 (red) base pairs this model will lead to similar dissociation but different association rates. Bottom: Two models of the final intercalated binding geometry of ΔΔ-**P** in a 14 A-T base pair duplex, with the bridging bidppz ligand positioned deeply in the minor groove. Compared to B-form DNA (left), DNA in A-form DNA (right) allows more favorable accommodation of the Ru-complex.

5.2.2 Unpaired Structures

Threading into poly(dAdT)$_2$ which, after thermal melting, had been rapidly re-annealed (giving back 73% duplex as determined from the UV hypochromicity) was showed in *Paper II* only to give a slight increase the intercalation rate. This indicated that presence of static, imperfectly paired structures is not a dominant factor in the fast intercalation of the AT polymer. Nevertheless, the introduction of particular structural deviations in AT-tract oligonucleotides may, as reported in *Paper V*, exert a significant influence on the interaction. We modified a 14 A-T base pair tract in three different ways: one in which a central A-T base pair is replaced by a C-C mismatch and two other

in which 2 and 14 additional A/T bases are inserted in one of the strands, creating a small bulge and a large loop, respectively. Association and dissociation kinetics of imperfect duplexes with ΔΔ-**P** at 25°C are shown in Figure 5.10.

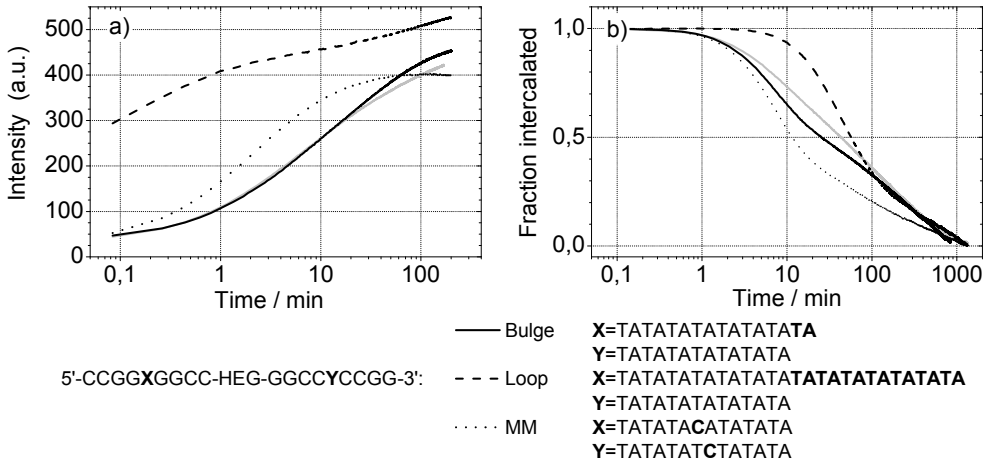

Figure 5.10 Interaction with unpaired DNA. (a) Luminescence intensity after mixing ΔΔ-**P** and HEG-linked oligonucleotides at 25°C. (b) Dissociation probed by poly(dAdT)$_2$ sequestering (equimolar amount) at 50°C. Y = 0 represent complete sequestering. Coding as indicated in figure. Fully paired 14 A-T base pair tract added for comparison (grey). Concentrations: [HEG-linked duplex] = 1 μM, [Ru complex] = 1 μM. Experiments performed in 150 mM NaCl, 1 mM sodium cacodylate buffer, pH 7.0. Note the different x-axis scales.

Code	Threading 25°C	Unthreading 50°C	Ratio
X=(TA)$_5$	n.d.[a]	65	0.37[b]
X=(TA)$_7$	6.0	43	7.2
(TA)$_7^{cc}$	1.6	11	7.0
(TA)$_{8:7}$	7.1	25	3.5
(TA)$_{14:7}$	<0.1	57	680

Table 5.3 Approximate half life (min) of ΔΔ-**P** threading and unthreading, determined from luminescence intensity change after mixing with DNA at 25°C and poly(dAdT)$_2$ sequestering at 50°C, respectively. [a]The very slow association makes estimation difficult. [b]Association $t_{1/2}$ at 37°C. Concentrations: [HEG-linked duplex] = 1 μM, [Ru complex] = 1 μM. Experiments performed in 150 mM NaCl, 1 mM sodium cacodylate buffer, pH 7.0.

Table 5.3 gives the estimated $t_{1/2}$ for association and dissociation, which also can be used to crudely assess the relative affinity. Even though these preliminary results need to be further explored before conclusions can be drawn with certainty, the results indicate that (1) small static openings in the form of mismatches increase the exchange rates without dramatically affecting the affinity, (2) small mobile bubbles in repeat sequences appear not to be the major rate-determining event and (3) large flexible openings can not only increase the threading rate considerably, but also stabilize the threaded state, leading to a large increase in affinity.

5.2.3 Supercoiling

As a step towards biologically more relevant DNA targets, we started to investigate the interaction between the threading dimers and superhelical DNA. It is a well-known phenomenon that negative supercoiling increases the affinity of intercalators.[23] Upon intercalation of ligands, negative superhelical turns are removed (σ is increased because Lk^0 is decreased), leading to a decrease in superhelical free energy that contributes to enhance binding. As more intercalator is progressively bound, the effect on the binding constant is decreased, eventually matching the binding constant for linear DNA at $\sigma = 0$. Figure 5.11 shows how the relative apparent binding constants for a supercoiled and linear topoisomer vary with ethidium bromide binding according to the method derived by Wu *et al.*[128] Even though the effect on the equilibrium constant is significant, it is generally too small to direct intercalators to supercoiled targets in a useful manner - even at low binding density.

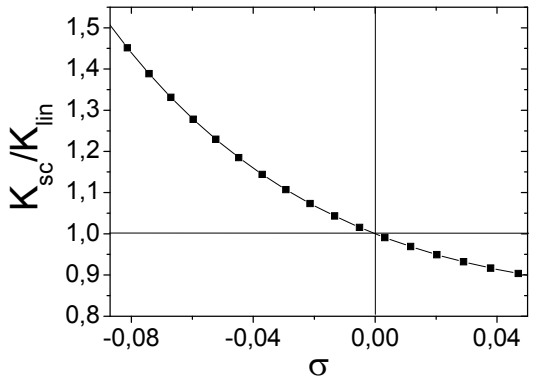

Figure 5.11 Relative ethidium binding constant for supercoiled and linear DNA as function of superhelix density σ. Ratio K_{sc}/K_{lin} determined from the binding isotherm ratio derived by Wu *et* al. for high-twist (σ = -0.083) supercoiled DNA with ethidium.[128]

In the last paper (VI) we used a 4331 base pair long plasmid DNA construct (T7 luc, $\sigma \approx$ -0.09) to study how target supercoiling influences the kinetics of binding of ΔΔ-**P**. The topological effect could easily be isolated from sequence effects by comparison to the plasmid DNA linearized by restriction enzymes. The construct contains a gene encoding luciferase under the transcriptional control of the T7 RNA polymerase promoter, which directly allowed us to study the effect of bound complex on a coupled transcription/translation system.

When mixing the linear form of T7 luc with ΔΔ-**P** at [ΔΔ-**P**]/[base pair] = 1/16 at 50°C, a slow increase in luminescence was observed, as expected, similar to that with calf thymus DNA at the same conditions. With the supercoiled form, however, the kinetic trace was remarkably different. The intensity increased rapidly after mixing, but arrested abruptly after 5 minutes at 1/3 of the final intensity, and proceeded into a phase of even

slower increase than for that of the linear form (Figure 5.12). At lower mixing ratio 1/64 with supercoiled DNA we obtained a trace in which the initial phase overlapped that at the high ratio, after which the intensity remained constant. The results suggest that the topological strain results in a biphasic behavior, where approximately 1 complex in 64 base pairs is allowed to intercalate rapidly, but that saturation above this threshold is kinetically hindered.

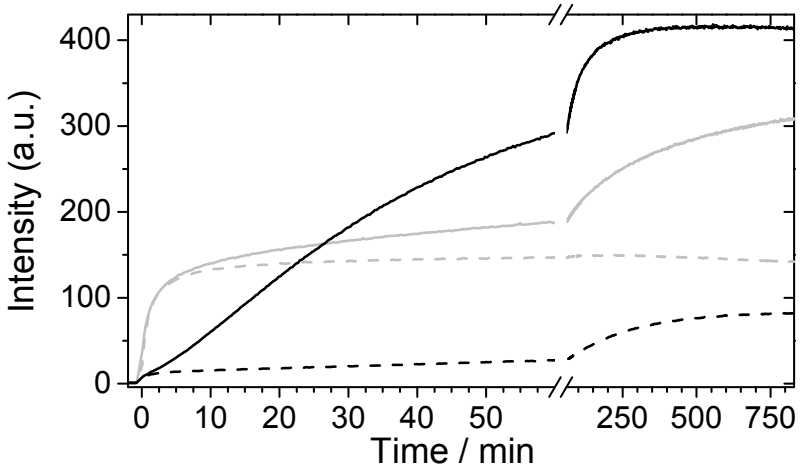

Figure 5.12 Kinetics of binding supercoiled DNA. Luminescence after mixing ΔΔ-**P** with linearized (black) and supercoiled (grey) T7 luc plasmid at 50°C at [ΔΔ-**P**]/[base pair] = 1/16 (—) or 1/64 (--). Experiments performed in 50 mM Tris, 100 mM NaCl, 10 mM $MgCl_2$, pH 7.5.

The pattern is evidently analogous to that for the equilibrium constant of intercalators with supercoiled DNA. The effect on the kinetics is however much larger. The $t_{1/2}$ is almost 2 orders of magnitude lower with the supercoiled topoisomer at low mixing ratio, to be compared with $K_{obs,sc}/K_{obs,lin} \approx 1.5$ for ethidium in the limit of low binding density. We further find it improbable that the threshold saturation behavior originates from complete relaxation of the DNA. An unwinding angle about eight times that of ethidium - approximately 200° - would be required to relax the DNA at ratio 1/64. This leads us to suggest that other structural factors may be involved. Analysis of plasmid sequence does not indicate that extrusion of specific alternative structures such as those mentioned in the introduction is very probable. It is however conceivable that the plasmid still contains "weaker" segments where intercalation is more probable. We know from the studies of unmatched oligonucleotides that threading can be drastically facilitated at unpaired sites. It is not unrealistic that such spots on the DNA are saturated at relatively low binding ratios.

5.3 Effect on gene expression

The plasmid construct can be utilized as a template for expression of firefly luciferase, an enzyme that catalyzes the ATP-dependent oxidation of a luciferin. The reaction produces light in proportion to the amount of luciferase, allowing estimation of the effectivness of the expression system. *Paper VI* reports the outcome of a series of measurements where the effect on transcription from the T7 luc plasmid by bound ligands was assessed by following the *in vitro* expression of luciferase.

T7 luc plasmid (supercoiled or linearized) was mixed with ΔΔ-**P** at [ΔΔ-**P**]/[base pair] = 1/50 and, either directly or after pre-incubation, added to the expression reaction mixture containing the necessary nucleotides, amino acids, enzymes and cofactors. The relative luciferase concentration with time was estimated from the chemoluminescence intensity by addition of a reaction mixture aliquot to the luciferase substrate solution every 20 min.

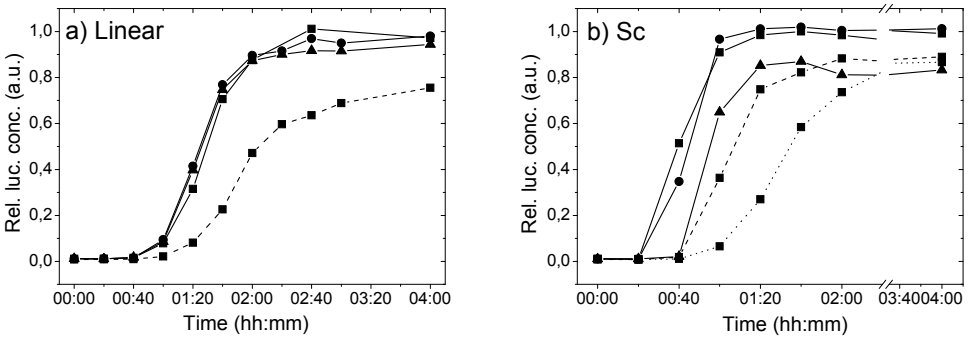

Figure 5.13 Transcription activity determined from luciferase luminescence with time after adding linear (a) or supercoiled (b) T7 luc template to reaction mixture. Relative concentration was determined from the mean of two measurements with 0.7 µg DNA alone (■) or DNA pre-mixed with ΔΔ-**P** at [complex]/[base pair] = 1/50 and added either instantly (●) or after incubation for 30 min at 50°C (▲) to the reaction mixture. Included as references are activity with 0.4 µg template DNA (**--**) and (for the supercoiled DNA) activity with template pre-mixed with actinomycin D at [ligand]/[base pair] = 1/50 (·····).

Luciferase production is more efficient from the naked supercoiled template, showing the importance of supercoiling in the transcriptional control (Figure 5.13). The slower production observed with reduced amount of DNA further shows that the accessibility of the template is rate determining in this interval. Short pre-incubation samples which, from the kinetic characterization, are expected only to give groove-bound ΔΔ-**P**, results in luciferase production that closely overlaps that of the naked template for the supercoiled as well as the linear plasmid. The findings indicate that the RNA polymerase displaces groove-bound complexes relatively easily. It also shows that presence of complex has small effects on the post-transcriptional steps. For samples pre-incubated with ΔΔ-**P** at elevated temperature, we expect that a large fraction are rearranged to the threaded state with the supercoiled but not the linear DNA. This

correlates with the observed luciferase concentration profile; with the supercoiled template we see a luciferase synthesis that is significantly delayed and reduced, whereas for the linear form it resembles that with the naked DNA. The transcriptional/translational assay thus indicates that the threaded binding mode constitutes a larger obstacle to the total RNA synthesis process than unthreaded external binding.

The inactivation at ratio 1/50 can be estimated to roughly correspond to a 30% reduction of the template available for transcription as judged from the production with reduced amount of template DNA. This effect is much smaller than that of actinomycin D at the same mixing ratio (see figure). ΔΔ-**P** may, like simpler intercalating and minor groove binding drugs, primarily interfere with initiation steps of transcription.[55] For such molecules, the unwinding and subsequent strand separation that occurs as the RNA polymerase approaches a binding site has been suggested to induce fast dissociation which reduces the effect on the elongation phase. Once dissociated, a re-associated complex will be kinetically trapped at the external binding mode, limiting further interference with the transcriptional machinery.

6. CONCLUDING REMARKS

The work presented in this Thesis shows the intriguing way in which DNA interactions in the test-tube – and probably also in the living cell - may be controlled. It demonstrates how the sequence dependent conformation of the DNA gives rise to kinetically favored reaction paths which in a slowly equilibrating system, here exemplified by the threading of a bulky, charged metal centre through the DNA duplex, can result in a high degree of selectivity. It has however also been learnt that interactions can be multifaceted and that identifying and mechanistically interpreting the important factors, an ultimate aim in this particular work, is complex. Still, a number of important conclusions can be drawn, summarized below:

- Both enantiomers of analogues **P** and **B** rearrange from groove-bound to threaded geometry in mixed sequences of DNA, but requires hours at elevated temperature to reach equilibrium. Alternating AT polymers, on the other hand, are intercalated within a few minutes at room temperature. The ratio of the forward rearrangement rates is estimated to vary between 65 (ΛΛ-**P**) and 2500 (ΛΛ-**B**).
- A systematic study with structurally well-defined hairpin oligonucleotides showed that the interval 10 to 14 alternating A-T base pairs is critical for efficient threading of **P** and **B**. This is a stretch of DNA considerably larger than the complexes themselves. The cooperativity of a conformational distortion around the site of interaction may be envisaged to communicate the distant sequence information.
- The threading rate of ΔΔ-**P** into a negatively supercoiled plasmid at low binding density is approximately two orders of magnitude higher than into the cleaved linear form. The accelerated intercalation leads to partial inhibition of luciferase expression from the supercoiled plasmid construct.
- The strong thermodynamic preference for long alternating AT-DNA can be utilized to probe the dissociation of ΔΔ-**P** and ΔΔ-**B** from mixed sequence DNA. Half-lives of dissociation are estimated to 38 and 18 h at physiological temperature, respectively. Access to dissociation kinetics allowed a complete thermodynamic characterization of the interaction with mixed sequence DNA, showing that the rearrangement from groove binding to intercalation is an entropically driven process.
- By analysis of the evolution of the CD-spectrum, the generally multiphasic emission increase can be divided into the actual threading and subsequent rearrangement processes. It reveals that threading of flexible **B** and **P** and the rigid dimeric ruthenium complex **F** into poly(dAdT)$_2$ follows pseudo 1st-order kinetics and thus can be described as a uni-molecular rearrangement. Threading

of the non-luminescent **S**, with smaller non-aromatic ancillary ligands, is more complex.

- From comparison of threading kinetics of **P** and **F** with poly(dAdT)$_2$ it is evident that the flexibility of the bridging ligand is an important factor. **S** threads considerably slower than **B** and **P** despite having smaller ancillary ligands, suggesting that hydrophobic ligands can promote the passage through the DNA.

The AT-selectivity demonstrated by the binuclear ruthenium complexes *in vitro* theoretically make them interesting as leads for new drugs against parasitic protozoa with AT-rich DNA, such as the malaria parasite *Plasmodium falciparum* (85% A+T) or *Trypanosoma bruncei* and the other closely related kinetoplastid parasites that cause trypanosomiasis and leishmaniasis. Several challanges remain, however. Naturally, the selectivity and activity in living cells have to be properly assessed. Telling from the limited number of reports on the *in vivo* activity, relatively little is known about the cytotoxicity of ruthenium polypyridyl complexes in general. One major obstacle for binuclear complexes can however directly be identified. Due to the high permanent charge, membrane penetration is poor as illustrated by the micrographs in Figure 6.1.

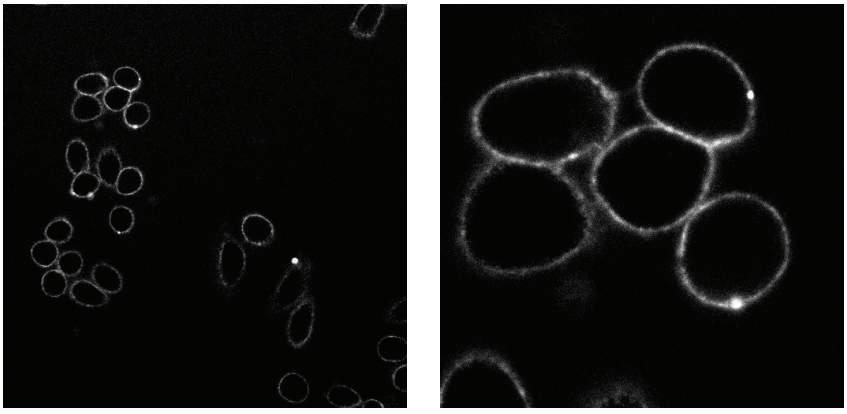

Figure 6.1 Confocal laser scanning microscopy imaging of binuclear ruthenium complex enriched in membrane of CHO-K1 cells, displaying the inability of the highly charged complexes to effectively diffuse to the nucleus.

Improved bioavailability could possibly be attained by reducing the net charge by use of negatively charged ligands, or by use of alternative metals such as rhenium(I). One could also imagine that the knowledge acquired from studies of ruthenium complexes eventually will aid the development metal-free threading agents exhibiting similar DNA binding characteristics. On a shorter term the binuclear ruthenium complexes could be optimized for use as *in vitro* site-selective luminescent probes of nucleic acids, with typical diagnostic applications in sequence analysis and mutation detection.

7. AUTHOR'S ACKNOWLEDGEMENTS

I am grateful to those of you who, directly or indirectly, contributed to this book

THANK YOU

PER for guidance based on curiosity, creativity and a unique wealth of knowledge. You have taught me to carry out research • BENGT for giving me an interesting and challenging task, co-supervision and for always being a source of inspiration • FREDRIK you picked me up and embraced me. Happy that you are back, boy • JOHN my mental coach in and outside the gym. I miss you a lot. F´s and J´s proofreading is also highly appreciated • MARCUS for support and encouragement throughout the project • TOM BROWN for collaboration and advice • ERIK J who through an excellent diploma work lead the project into a new exciting area • My dear room-mate KRISTINA for friendship, collaboration and advice on various matters • ANNA R for co-authorship, help with figures and for keeping me on my toes • JOHANNA, FRIDA and all other RU-GROUP MEMBERS • ANNA, ERICA, GUNILLA and GUNNAR for all help during the years • To past and present, 5th-floor and MC2, COLLEAGUES for the open, creative and fun atmosphere that I always will associate with my years at Physical Chemistry. Times of fika, innebandy, after works, conference-trips and karaoke sessions are precious memories • My FRIENDS and FAMILY, of course • JONNY and BIRGITTA deserve a special thanks for helping us during times of thesis-writing • And at last, kisses to them whom I love the most: SOFIA, MÄRTA & INGMAR

8. REFERENCES

(1) Watson, J. D.; Crick, F. H. C. Molecular structure of nucleic acids. A structure for deoxyribose nucleic acid *Nature* **1953**, 737-738.

(2) Lander, E. S. *et al.* Initial sequencing and analysis of the human genome *Nature* **2001**, *409*, 860-921.

(3) Drew, H. R.; Wing, R. M.; Takano, T.; Broka, C.; Tanaka, S.; Itakura, K.; Dickerson, R. E. Structure of a B-DNA Dodecamer: Conformation and Dynamics *Proceedings of the National Academy of Sciences of the United States of America-Biological Sciences* **1981**, *78*, 2179-2183.

(4) Dickerson, R. E.; Drew, H. R. Structure of a B-DNA Dodecamer II. Influence of Base Sequence on Helix Structure *Journal of Molecular Biology* **1981**, *149*, 761-786.

(5) Yanagi, K.; Prive, G. G.; Dickerson, R. E. Analysis of Local Helix Geometry in 3 B-DNA Decamers and 8 Dodecamers *Journal of Molecular Biology* **1991**, *217*, 201-214.

(6) Berman, H. M.; Olson, W. K.; Beveridge, D. L.; Westbrook, J.; Gelbin, A.; Demeny, T.; Hsieh, S. H.; Srinivasan, A. R.; Schneider, B. The Nucleic-Acid Database - A Comprehensive Relational Database of 3-Dimensional Structures of Nucleic-Acids *Biophysical Journal* **1992**, *63*, 751-759.

(7) Grzeskowiak, K. Sequence-dependent structural variation in B-DNA *Chemistry & Biology* **1996**, *3*, 785-790.

(8) Suzuki, M.; Yagi, N.; Finch, J. T. Role of base-backbone and base-base interactions in alternating DNA conformations *Febs Letters* **1996**, *379*, 148-152.

(9) Yoon, C.; Prive, G. G.; Goodsell, D. S.; Dickerson, R. E. Structure of an Alternating-B DNA Helix and Its Relationship to A-Tract DNA *Proceedings of the National Academy of Sciences of the United States of America* **1988**, *85*, 6332-6336.

(10) Chen, K. K.; Donelson, J. E. Sequences of 2 Kinetoplast DNA Minicircles of Trypanosoma-Brucei *Proceedings of the National Academy of Sciences of the United States of America-Biological Sciences* **1980**, *77*, 2445-2449.

(11) Barrois, M.; Riou, G.; Galibert, F. Complete Nucleotide-Sequence of Minicircle Kinetoplast DNA from Trypanosoma-Equiperdum *Proceedings of the National Academy of Sciences of the United States of America-Biological Sciences* **1981**, *78*, 3323-3327.

(12) Marini, J. C.; Levene, S. D.; Crothers, D. M.; Englund, P. T. Bent Helical Structure in Kinetoplast DNA *Proceedings of the National Academy of Sciences of the United States of America-Biological Sciences* **1982**, *79*, 7664-7668.

(13) Ohyama, T. Intrinsic DNA bends: an organizer of local chromatin structure for transcription *Bioessays* **2001**, *23*, 708-715.

(14) Yuan, H.; Quintana, J.; Dickerson, R. E. Alternative Structures for Alternating Poly(dA-dT) Tracts: The Structure of the B-DNA Decamer C-G-A-T-A-T-A-T-C-G *Biochemistry* **1992**, *31*, 8009-8021.

(15) Klug, A.; Jack, A.; Viswamitra, M. A.; Kennard, O.; Shakked, Z.; Steitz, T. A. Hypothesis on a Specific Sequence-Dependent Conformation of DNA and Its Relation to the Binding of the Lac-Repressor Protein *Journal of Molecular Biology* **1979**, *131*, 669-680.

(16) Churchill, M. E. A.; Travers, A. A. Protein Motifs That Recognize Structural Features of DNA *Trends in Biochemical Sciences* **1991**, *16*, 92-97.

(17) Svozil, D.; Kalina, J.; Omelka, M.; Schneider, B. DNA conformations and their sequence preferences *Nucleic Acids Research* **2008**, *36*, 3690-3706.

(18) Nikolov, D. B.; Chen, H.; Halay, E. D.; Hoffmann, A.; Roeder, R. G.; Burley, S. K. Crystal structure of a human TATA box-binding protein/TATA element complex *Proceedings of the National Academy of Sciences of the United States of America* **1996**, *93*, 4862-4867.

(19) Juo, Z. S.; Chiu, T. K.; Leiberman, P. M.; Baikalov, I.; Berk, A. J.; Dickerson, R. E. How proteins recognize the TATA box *Journal of Molecular Biology* **1996**, *261*, 239-254.
(20) Davis, N. A.; Majee, S. S.; Kahn, J. D. TATA box DNA deformation with and without the TATA box-binding protein *Journal of Molecular Biology* **1999**, *291*, 249-265.
(21) Lodish, H. F. *Molecular cell biology*, 4. ed.; W. H. Freeman and Co.: New York, 2000.
(22) Françon, P.; Méchali, M. DNA Replication Origins **2006** In: Encyclopedia of Life Sciences, John Wiley & Sons Ltd, Chichester. http://www.els.net/.
(23) Vinograd, J.; Lebowitz, J.; Radloff, R.; Watson, R.; Laipis, P. Twisted Circular Form of Polyoma Viral DNA *Proceedings of the National Academy of Sciences of the United States of America* **1965**, *53*, 1104-1111.
(24) Vologodskii, A.; Cozzarelli, N. R. Effect of supercoiling on the juxtaposition and relative orientation of DNA sites *Biophysical Journal* **1996**, *70*, 2548-2556.
(25) Echols, H. Nucleoprotein Structures Initiating DNA-Replication, Transcription, and Site-Specific Recombination *Journal of Biological Chemistry* **1990**, *265*, 14697-14700.
(26) Frank-Kamenetskii, M. D. DNA Supercoiling and Unusual Structures. In *DNA topology and its biological effects*; Nicholas R. Cozzarelli, J. C. W., Ed.; Cold Spring Harbor Laboratory Press: Cold Spring Harbor, NY, 1990; pp 185-215.
(27) Palecek, E. Local Supercoil-Stabilized DNA Structures *Critical Reviews in Biochemistry and Molecular Biology* **1991**, *26*, 151-226.
(28) McClellan, J. A.; Lilley, D. M. J. A Two-State Conformational Equilibrium for Alternating (A-T)n Sequences in Negatively Supercoiled DNA *Journal of Molecular Biology* **1987**, *197*, 707-721.
(29) Peck, L. J.; Nordheim, A.; Rich, A.; Wang, J. C. Flipping of Cloned d(pCpG)n*d(pCpG)n DNA-Sequences from Right-Handed to Left-Handed Helical Structure by Salt, Co(III), or Negative Supercoiling *Proceedings of the National Academy of Sciences of the United States of America-Biological Sciences* **1982**, *79*, 4560-4564.
(30) Htun, H.; Dahlberg, J. E. Single Strands, Triple Strands, and Kinks in H-DNA *Science* **1988**, *241*, 1791-1796.
(31) Bloomfield, V. A.; Crothers, D. M.; Tinoco, I. *Nucleic acids: Structures, Properties, and Functions*; University Science Books: Sausalito, California, 2000.
(32) Stuart, M. J.; Nagel, R. L. Sickle-cell disease *Lancet* **2004**, *364*, 1343-1360.
(33) Cheung, J. C.; Deber, C. M. Misfolding of the cystic fibrosis transmembrane conductance regulator and disease *Biochemistry* **2008**, *47*, 1465-1473.
(34) Jacob, S.; Praz, F. DNA mismatch repair defects: role in colorectal carcinogenesis *Biochimie* **2002**, *84*, 27-47.
(35) Wang, Y. H.; Griffith, J. Effects of Bulge Composition and Flanking Sequence on the Kinking of DNA by Bulged Bases *Biochemistry* **1991**, *30*, 1358-1363.
(36) Cotton, R. G. H. Mutation Detection **2006** In: Encyclopedia of Life Sciences, John Wiley & Sons Ltd, Chichester. http://www.els.net/.
(37) Hacia, J. G. Resequencing and mutational analysis using oligonucleotide microarrays *Nature Genetics* **1999**, *21*, 42-47.
(38) Syvänen, A.-C. Microarrays: Use in Mutation Detection **2005** In: Encyclopedia of Life Sciences, John Wiley & Sons Ltd, Chichester. http://www.els.net/.
(39) Bui, C. T.; Rees, K.; Lambrinakos, A.; Bedir, A.; Cotton, R. G. H. Site-selective reactions of imperfectly matched DNA with small chemical molecules: applications in mutation detection *Bioorganic Chemistry* **2002**, *30*, 216-232.
(40) Kopka, M. L.; Yoon, C.; Goodsell, D.; Pjura, P.; Dickerson, R. E. The Molecular-Origin of DNA Drug Specificity in Netropsin and Distamycin *Proceedings of the National Academy of Sciences of the United States of America* **1985**, *82*, 1376-1380.
(41) Abu-Daya, A.; Brown, P. M.; Fox, K. R. DNA sequence preferences of several AT-selective minor groove binding ligands *Nucleic Acids Research* **1995**, *23*, 3385-3392.
(42) Abu-Daya, A.; Fox, K. R. Interaction of minor groove binding ligands with long AT tracts *Nucleic Acids Research* **1997**, *25*, 4962-4969.

(43) Kubista, M.; Åkerman, B.; Nordén, B. Characterization of Interaction between DNA and 4',6-Diamidino-2-Phenylindole by Optical Spectroscopy *Biochemistry* **1987**, *26*, 4545-4553.
(44) Wilson, W. D.; Tanious, F. A.; Barton, H. J.; Jones, R. L.; Fox, K.; Wydra, R. L.; Strekowski, L. DNA sequence dependent binding modes of 4',6-diamidino-2-phenylindole (DAPI) *Biochemistry* **1990**, *29*, 8452-8461.
(45) Eriksson, S.; Kim, S. K.; Kubista, M.; Nordén, B. Binding of 4',6-Diamidino-2-Phenylindole (DAPI) to AT Regions of DNA - Evidence for an Allosteric Conformational Change *Biochemistry* **1993**, *32*, 2987-2998.
(46) Reinhardt, C. G.; Krugh, T. R. A comparative study of ethidium bromide complexes with dinucleotides and DNA: direct evidence for intercalation and nucleic acid sequence preferences *Biochemistry* **1978**, *17*, 4845-4854.
(47) Becker, H. C.; Nordén, B. DNA binding properties of 2,7-diazapyrene and its N-methylated cations studied by linear and circular dichroism spectroscopy and calorimetry *Journal of the American Chemical Society* **1997**, *119*, 5798-5803.
(48) Graves, D. E.; Velea, L. M. Intercalative binding of small molecules to nucleic acids *Current Organic Chemistry* **2000**, *4*, 915-929.
(49) Oda, N.; Nakamura, H. Thermodynamic and kinetic analyses for understanding sequence-specific DNA recognition *Genes to Cells* **2000**, *5*, 319-326.
(50) Lerman, L. S. Structural Considerations in Interaction of DNA and Acridines *Journal of Molecular Biology* **1961**, *3*, 18-30.
(51) Helene, C. DNA recognition - Reading the minor groove *Nature* **1998**, *391*, 436-438.
(52) Chen, F. M. Kinetic and Equilibrium Binding-Studies of Actinomycin-D with Some d(TGCA)-Containing Dodecamers *Biochemistry* **1988**, *27*, 1843-1848.
(53) Robinson, H.; Gao, Y. G.; Yang, X. L.; Sanishvili, R.; Joachimiak, A.; Wang, A. H. J. Crystallographic analysis of a novel complex of actinomycin D bound to the DNA decamer CGATCGATCG *Biochemistry* **2001**, *40*, 5587-5592.
(54) Sobell, H. M. Actinomycin and DNA-Transcription *Proceedings of the National Academy of Sciences of the United States of America* **1985**, *82*, 5328-5331.
(55) Straney, D. C.; Crothers, D. M. Effect of Drug-DNA Interactions Upon Transcription Initiation at the lac Promoter *Biochemistry* **1987**, *26*, 1987-1995.
(56) Piestrzeniewicz, M.; Studzian, K.; Wilmanska, D.; Plucienniczak, G.; Gniazdowski, M. Effect of DNA-interacting drugs on phage T7 RNA polymerase *Acta Biochimica Polonica* **1998**, *45*, 127-132.
(57) Gao, Q.; Williams, L. D.; Egli, M.; Rabinovich, D.; Chen, S. L.; Quigley, G. J.; Rich, A. Drug-Induced DNA-Repair - X-Ray Structure of a DNA-Ditercalinium Complex *Proceedings of the National Academy of Sciences of the United States of America* **1991**, *88*, 2422-2426.
(58) Crow, S. D. G.; Bailly, C.; Garbay-Jaureguiberry, C.; Roques, B.; Shaw, B. R.; Waring, M. J. DNA sequence recognition by the antitumor drug ditercalinium *Biochemistry* **2002**, *41*, 8672-8682.
(59) Fox, K. R.; Waring, M. J. Evidence of Different Binding-Sites for Nogalamycin in DNA Revealed by Association Kinetics *Biochimica Et Biophysica Acta* **1984**, *802*, 162-168.
(60) Fox, K. R.; Brassett, C.; Waring, M. J. Kinetics of Dissociation of Noglamycin from DNA - Comparison with Other Anthracycline Antibiotics *Biochimica Et Biophysica Acta* **1985**, *840*, 383-392.
(61) Gao, Y. G.; Liaw, Y. C.; Robinson, H.; Wang, A. H. Binding of the antitumor drug nogalamycin and its derivatives to DNA: structural comparison *Biochemistry* **1990**, *29*, 10307-10316.
(62) Egli, M.; Williams, L. D.; Frederick, C. A.; Rich, A. DNA-nogalamycin interactions *Biochemistry* **1991**, *30*, 1364-1372.
(63) Tanious, F. A.; Yen, S. F.; Wilson, W. D. Kinetic and Equilibrium-Analysis of a Threading Intercalation Mode - DNA-Sequence and Ion Effects *Biochemistry* **1991**, *30*, 1813-1819.
(64) Tse, W. C.; Boger, D. L. Sequence-Selective DNA Recognition: Natural Products and Nature´s Lesson *Chemistry & Biology* **2004**, *11*, 1607-1617.

(65) Galm, U.; Hager, M. H.; Van Lanen, S. G.; Ju, J. H.; Thorson, J. S.; Shen, B. Antitumor antibiotics: Bleomycin, endiynes, and mitomycin *Chemical Reviews* **2005**, *105*, 739-758.
(66) Fivelman, Q. L.; Yardley, V.; Sutherland, C. J. Antiprotozoan Drugs **2009** In: Encyclopedia of Life Sciences, John Wiley & Sons Ltd, Chichester. http://www.els.net/.
(67) Boykin, D. W. Antimicrobial activity of the DNA minor groove binders furamidine and analogs *Journal of Brazilian Chemical Society* **2002**, *13*, 763-771.
(68) Mallena, S.; Lee, M. P. H.; Bailly, C.; Neidle, S.; Kumar, A.; Boykin, D. W.; Wilson, W. D. Thiophene-based diamidine forms a "super" AT binding minor groove agent *Journal of the American Chemical Society* **2004**, *126*, 13659-13669.
(69) Miao, Y.; Lee, M. P. H.; Parkinson, G. N.; Batista-Parra, A.; Ismail, M. A.; Neidle, S.; Boykin, D. W.; Wilson, W. D. Out-of-shape DNA minor groove binders: induced fit interactions of heterocyclic dications with the DNA minor groove *Biochemistry* **2005**, *44*, 14701-14708.
(70) Wilson, D. W.; Nguyen, B.; Tanious, F. A.; Mathis, A.; Hall, J. E.; Stephens, C. E.; Boykin, D. W. Dications that target the DNA minor groove: compound design and perparation, DNA interactions, cellular distribution and biological activity *Current Medicinal Chemistry - Anti-Cancer Agents* **2005**, *5*, 389-408.
(71) Klingbeil, M. M.; Drew, M. E.; Liu, Y. N.; Morris, J. C.; Motyka, S. A.; Saxowsky, T. T.; Wang, Z. F.; Englund, P. T. Unlocking the secrets of trypanosome kinetoplast DNA network replication *Protist* **2001**, *152*, 255-262.
(72) Mrksich, M.; Parks, M. E.; Dervan, P. B. Hairpin Peptide Motif. A New Class of Oligopeptides for Sequence-Specific Recognition in the Minor Groove of Double-Helical DNA *Journal of the American Chemical Society* **1994**, *116*, 7983-7988.
(73) White, S.; Szewczyk, J. W.; Turner, J. M.; Baird, E. E.; Dervan, P. B. Recognition of the four Watson-Crick base pairs in the DNA minor groove by synthetic ligands *Nature* **1998**, *391*, 468-471.
(74) Winters, T. A. Gene targeted agents: New oppotunities for rational drug development *Current Opinion in Molecular Therapeutics* **2000**, *2*, 670-681.
(75) Dervan, P. B. Molecular recognition of DNA by small molecules *Bioorganic & Medicinal Chemistry* **2001**, *9*, 2215-2235.
(76) Trauger, J. W.; Baird, E. E.; Dervan, P. B. Recognition of 16 base pairs in the minor groove of DNA by a pyrrole-imidazole polyamide dimer *Journal of the American Chemical Society* **1998**, *120*, 3534-3535.
(77) Fechter, E. J.; Olenyuk, B.; Dervan, P. B. Design of a sequence-specific DNA bisintercalator *Angewandte Chemie-International Edition* **2004**, *43*, 3591-3594.
(78) Dickinson, L. A.; Burnett, R.; Melander, C.; Edelson, B. S.; Arora, P. S.; Dervan, P. B.; Gottesfeld, J. M. Arresting cancer proliferation by small-molecule gene regulation *Chemistry & Biology* **2004**, *11*, 1583-1594.
(79) Vos, J. G.; Kelly, J. M. Ruthenium polypyridyl chemistry; from basic research to applications and back again *Dalton Transactions* **2006**, 4869-4883.
(80) Barton, J. K.; Danishefsky, A.; Goldberg, J. Tris(phenanthroline)ruthenium(II): stereoselectivity in binding to DNA *J. Am. Chem. Soc.* **1984**, *106*, 2172-2176.
(81) Kumar, C. V.; Barton, J. K.; Turro, N. J. Photophysics of Ruthenium Complexes Bound to Double Helical DNA *Journal of the American Chemical Society* **1985**, *107*, 5518-5523.
(82) Barton, J. K.; Goldberg, J. M.; Kumar, C. V.; Turro, N. J. Binding Modes and Base Specificity of Tris(Phenanthroline)Ruthenium(II) Enantiomers with Nucleic-Acids - Tuning the Stereoselectivity *Journal of the American Chemical Society* **1986**, *108*, 2081-2088.
(83) Rehmann, J. P.; Barton, J. K. H-1-NMR Studies of Tris(Phenanthroline) Metal-Complexes Bound to Oligonucleotides - Characterization of Binding Modes *Biochemistry* **1990**, *29*, 1701-1709.
(84) Hiort, C.; Nordén, B.; Rodger, A. Enantiopreferential DNA-Binding of [Ru(II)(1,10-Phenanthroline)3]2+ Studied with Linear and Circular-Dichroism *Journal of the American Chemical Society* **1990**, *112*, 1971-1982.

(85) Satyanarayana, S.; Dabrowiak, J. C.; Chaires, J. B. Neither delta- nor lambda-tris(phenanthroline)ruthenium(II) binds to DNA by classical intercalation *Biochemistry* **1992**, *31*, 9319-9324.

(86) Satyanarayana, S.; Dabrowiak, J. C.; Chaires, J. B. Tris(phenanthroline)ruthenium(II) enantiomer interactions with DNA: mode and specificity of binding *Biochemistry* **1993**, *32*, 2573-2584.

(87) Eriksson, M.; Leijon, M.; Hiort, C.; Nordén, B.; Gräslund, A. Binding of Delta-[Ru(Phen)3]2+ and Lambda-[Ru(Phen)3]2+ to [d(CGCGATCGCG)]2 Studied by NMR *Biochemistry* **1994**, *33*, 5031-5040.

(88) Lincoln, P.; Nordén, B. DNA Binding Geometries of Ruthenium(II) Complexes with 1,10-Phenanthroline and 2,2'-Bipyridine Ligands Studied with Linear Dichroism Spectroscopy. Borderline Cases of Intercalation *Journal of Physical Chemistry B* **1998**, *102*, 9583-9594.

(89) Chambron, J. C.; Sauvage, J. P.; Amouyal, E.; Koffi, P. Ru(Bipy)2 (Dipyridophenazine)2+ - A Complex with a Long-Range Directed Charge-Transfer Excited-State *Nouveau Journal De Chimie-New Journal of Chemistry* **1985**, *9*, 527-529.

(90) Friedman, A. E.; Chambron, J. C.; Sauvage, J. P.; Turro, N. J.; Barton, J. K. Molecular Light Switch for DNA - Ru(bpy)2(dppz)2+ *Journal of the American Chemical Society* **1990**, *112*, 4960-4962.

(91) Jenkins, Y.; Friedman, A. E.; Turro, N. J.; Barton, J. K. Characterization of Dipyridophenazine Complexes of Ruthenium(II) - the Light Switch Effect as a Function of Nucleic-Acid Sequence and Conformation *Biochemistry* **1992**, *31*, 10809-10816.

(92) Dupureur, C. M.; Barton, J. K. Use of Selective Deuteration and 1H NMR in Demonstrating Major Groove Binding of Delta-[Ru(phen)2dppz]2+ to d(GTCGAC)2 *Journal of the American Chemical Society* **1994**, *116*, 10286-10287.

(93) Lincoln, P.; Broo, A.; Nordén, B. Diastereomeric DNA-binding geometries of intercalated ruthenium(II) trischelates probed by linear dichroism: [Ru(phen)2DPPZ]2+ and [Ru(phen)2BDPPZ]2+ *Journal of the American Chemical Society* **1996**, *118*, 2644-2653.

(94) Tuite, E.; Lincoln, P.; Nordén, B. Photophysical evidence that Delta- and Lambda-[Ru(phen)2(dppz)]2+ intercalate DNA from the minor groove *Journal of the American Chemical Society* **1997**, *119*, 239-240.

(95) Holmlin, R. E.; Stemp, E. D. A.; Barton, J. K. Ru(phen)(2)dppz(2+) luminescence: Dependence on DNA sequences and groove-binding agents *Inorganic Chemistry* **1998**, *37*, 29-34.

(96) Hiort, C.; Lincoln, P.; Nordén, B. DNA-Binding of Delta-[Ru(Phen)2dppz]2+ and Lambda-[Ru(Phen)2dppz]2+ *Journal of the American Chemical Society* **1993**, *115*, 3448-3454.

(97) Chaires, J. B. A thermodynamic signature for drug-DNA binding mode *Archives of Biochemistry and Biophysics* **2006**, *453*, 26-31.

(98) Haq, I.; Lincoln, P.; Suh, D. C.; Norden, B.; Chowdhry, B. Z.; Chaires, J. B. Interaction of Delta-[Ru(Phen)2Dppz]2+ and Lambda-[Ru(Phen)2Dppz]2+ with DNA - A Calorimetric and Equilibrium Binding Study *Journal of the American Chemical Society* **1995**, *117*, 4788-4796.

(99) Nordén, B.; Lincoln, P.; Åkerman, B.; Tuite, E. DNA interactions with substitution-inert transition metal ion complexes *Metal Ions in Biological Systems* **1996**, *33*, 177-252.

(100) Erkkila, K. E.; Odom, D. T.; Barton, J. K. Recognition and Reaction of Metallointercalators with DNA *Chemical Reviews (Washington, D. C.)* **1999**, *99*, 2777-2795.

(101) Metcalfe, C.; Thomas, J. A. Kinetically inert transition metal complexes that reversibly bind to DNA *Chemical Society Reviews* **2003**, *32*, 215-224.

(102) Pierard, F.; Kirsch-De Mesmaeker, A. Bifunctional transition metal complexes as nucleic acid photoprobes and photoreagents *Inorganic Chemistry Communications* **2006**, *9*, 111-126.

(103) Foxon, S. P.; Phillips, T.; Gill, M. R.; Towrie, M.; Parker, A. W.; Webb, M.; Thomas, J. A. A multifunctional light switch: DNA binding and cleavage

properties of a heterobimetallic ruthenium-rhenium dipyridophenazine complex *Angewandte Chemie-International Edition* **2007**, *46*, 3686-3688.
(104) Zeglis, B. M.; Barton, J. K. A mismatch-selective bifunctional rhodium-oregon green conjugate: A fluorescent probe for mismatched DNA *Journal of the American Chemical Society* **2006**, *128*, 5654-5655.
(105) Zeglis, B. M.; Boland, J. A.; Barton, J. K. Targeting abasic sites and single base bulges in DNA with metalloinsertors *Journal of the American Chemical Society* **2008**, *130*, 7530-7531.
(106) Önfelt, B.; Lincoln, P.; Nordén, B. A Molecular Staple for DNA: Threading Bis-intercalating [Ru(phen)2dppz]2+ Dimer *Journal of the American Chemical Society* **1999**, *121*, 10846-10847.
(107) Önfelt, B.; Lincoln, P.; Nordén, B. Enantioselective DNA threading dynamics by phenazine-linked *Journal of the American Chemical Society* **2001**, *123*, 3630-3637.
(108) Önfelt, B. *Chiral ruthenium dipyridophenazine complexes: DNA binding and excited state relaxation*; Chalmers University of Technology: Gothenburg, 2002.
(109) Fox, K. R.; Waring, M. J. Evidence of different binding sites for nogalamycin in DNA revealed by association kinetics *Biochimica Et Biophysica Acta* **1984**, *802*, 162-168.
(110) Lincoln, P.; Nordén, B. Binuclear ruthenium(II) phenanthroline compounds with extreme binding affinity for DNA *Chemical Communications* **1996**, 2145-2146.
(111) Wilhelmsson, L. M.; Westerlund, F.; Lincoln, P.; Nordén, B. DNA-Binding of Semirigid Binuclear Ruthenium Complex Delta,Delta-[mu-(11,11'-bidppz)(phen)4Ru2]4+: Extremely Slow Intercalation Kinetics *Journal of the American Chemical Society* **2002**, *124*, 12092-12093.
(112) Wilhelmsson, L. M.; Esbjörner, E. K.; Westerlund, F.; Nordén, B.; Lincoln, P. Meso stereoisomer as a probe of enantioselective threading intercalation of semirigid ruthenium complex [mu-(11,11'-bidppz)(phen)4Ru2]4+ *Journal of Physical Chemistry B* **2003**, *107*, 11784-11793.
(113) Cantor, C. R.; Schimmel, P. R. *Biophysical chemistry*; Freeman: San Francisco, 1980.
(114) Lakowicz, J. R. *Principles of fluorescence spectroscopy*, 3. ed.; Springer: New York, 2006.
(115) Önfelt, B.; Olofsson, J.; Lincoln, P.; Nordén, B. Picosecond and Steady-State Emission of [Ru(phen)2dppz]2+ in Glycerol: Anomalous Temperature Dependence *Journal of Physical Chemistry A* **2003**, *107*, 1000-1009.
(116) Olofsson, J.; Önfelt, B.; Lincoln, P. Three-state light switch of [Ru(phen)(2)dppz](2+): Distinct excited-state species with two, one, or no hydrogen bonds from solvent *Journal of Physical Chemistry A* **2004**, *108*, 4391-4398.
(117) Nordén, B.; Kubista, M.; Kurucsev, T. Linear dichroism spectroscopy of nucleic acids *Quarterly Reviews of Biophysics* **1992**, *25*, 51-170.
(118) Rodger, A.; Nordén, B. *Circular dichroism and linear dichroism*; Oxford Univ. Press: Oxford, 1997.
(119) Arrhenius, S. A. Über die Reaktionsgeschwindigkeit bei der Inversion von Rohrzucker durch Säuren *Zeitschrift für physikalische Chemie* **1889**, *4*, 226-248.
(120) Levine, I. N. *Physical chemistry*, 4. ed.; McGraw-Hill: New York, 1995.
(121) Oshikiri, T.; Takashima, Y.; Yamaguchi, H.; Harada, A. Kinetic control of threading of cyclodextrins onto axle molecules *Journal of the American Chemical Society* **2005**, *127*, 12186-12187.
(122) Mcghee, J. D.; Hippel, P. H. V. Theoretical Aspects of DNA-Protein Interactions - Cooperative and Non-Cooperative Binding of Large Ligands to a One-Dimensional Homogeneous Lattice *Journal of Molecular Biology* **1974**, *86*, 469-489.
(123) Nordell, P. *DNA Binding of Bidppz Ruthenium Complexes - Effect of Ancillary Ligands on Binding Modes and Kinetics*; Chalmers University of technology: Gothenburg, 2003.
(124) Westerlund, F.; Wilhelmsson, L. M.; Nordén, B.; Lincoln, P. Micelle-Sequestered Dissociation of Cationic DNA-Intercalated Drugs: Unexpected Surfactant-

Induced Rate Enhancement *Journal of the American Chemical Society* **2003**, *125*, 3773-3779.

(125) Paramanathan, T.; Westerlund, F.; McCauley, M. J.; Rouzina, I.; Lincoln, P.; Williams, M. C. Mechanically Manipulating the DNA Threading Intercalation Rate *Journal of the American Chemical Society* **2008**, *130*, 3752-3753.

(126) McClellan, J. A.; Palecek, E.; Lilley, D. M. J. (A-T)n Tracts Embedded in Random Sequence DNA - Formation of a Structure Which Is Chemically Reactive and Torsionally Deformable *Nucleic Acids Research* **1986**, *14*, 9291-9309.

(127) Lane, M. J.; Laplante, S.; Rehfuss, R. P.; Borer, P. N.; Cantor, C. R. Actinomycin-D Facilitates Transition of AT Domains in Molecules of Sequence (AT)nAGCT(AT)n to a DNase-I Detectable Alternating Structure *Nucleic Acids Research* **1987**, *15*, 839-852.

(128) Wu, P. G.; Song, L.; Clendenning, J. B.; Fujimoto, B. S.; Benight, A. S.; Schurr, J. M. Interaction of Chloroquine with Linear and Supercoiled DNAs - Effect on the Torsional Dynamics, Rigidity, and Twist Energy Parameter *Biochemistry* **1988**, *27*, 8128-8144.